

AD-A040 234

ARMY COMMUNICATIONS-ELECTRONICS ENGINEERING INSTALLAT--ETC F/G 17/2.1
DIGITAL TRANSMISSION EVALUATION PROJECT DR8A TEST.(U)

APR 77 J E HAMANT, O P CONNELL, H S WALCZYK

UNCLASSIFIED

CCC-CED-77-DTEP-012

NL

| OF |

AD A040234



END
DATE
FILMED
7-77

ADA 040234

CCC-CED-77-DTEP-012

DIGITAL TRANSMISSION EVALUATION PROJECT
DR&A TEST
FINAL REPORT

C
B.S.

CPT JAMES E. HAMANT
O. P. CONNELL
HENRY S. WALCZYK

DDC
JUN 7 1977
C

APRIL 1977

Approved for public release; distribution unlimited

AD No. _____
DDC FILE COPY

HEADQUARTERS
US ARMY COMMUNICATIONS-ELECTRONICS ENGINEERING INSTALLATION AGENCY
Fort Huachuca, Arizona 85613

DISTRIBUTION STATEMENT

Approved for public release

Distribution unlimited

DISPOSITION INSTRUCTIONS

Destroy this document when no longer needed

Do not return it to the originator

DISCLAIMER

The findings in this report are not to be construed as an official Department of the Army position unless so designated by other authorized documents.

The use of trade names in this document does not constitute an official endorsement or approval of the use of such commercial hardware or software. This document may not be cited for purpose of advertisement.

ACQUISITION FOR		
NTIS	White Section	<input checked="" type="checkbox"/>
DDC	Self Section	<input type="checkbox"/>
UNANNOUNCED		<input type="checkbox"/>
JUSTIFICATION		
BY		
DISTRIBUTION/AVAILABILITY CODES		
Dist.	Avail.	or SPECIAL
A		

SECURITY CLASSIFICATION OF THIS PAGE (When Data Entered)

REPORT DOCUMENTATION PAGE		READ INSTRUCTIONS BEFORE COMPLETING FORM
1. REPORT NUMBER 14 CCC-CED-77-DTEP-012 ✓	2. GOVT ACCESSION NO.	3. RECIPIENT'S CATALOG NUMBER
4. TITLE (and Subtitle) 6 Digital Transmission Evaluation Project DRBA Test, Final Report		5. TYPE OF REPORT & PERIOD COVERED 9 Final Report, May 75-Feb 77
7. AUTHOR(s) 13 James E. Hamant, O. P. Connelly, USACE/SA Henry S. Walczyk, USACE/SA		6. CONTRACT OR GRANT NUMBER(s) GCC-CED-77-DTEP-012
9. PERFORMING ORGANIZATION NAME AND ADDRESS US Army Communications-Electronics Engineering Installation Agency & US Army Electronic Proving Ground, Fort Huachuca, AZ 85613 ✓		10. PROGRAM ELEMENT, PROJECT, TASK AREA & WORK UNIT NUMBERS
11. CONTROLLING OFFICE NAME AND ADDRESS US Army Communications Command, Assistant Chief of Staff for Force Development, Fort Huachuca, AZ 85613		12. REPORT DATE 14 30 April 1977
14. MONITORING AGENCY NAME & ADDRESS (if different from Controlling Office) US Army Communications Systems Agency Fort Monmouth, NJ 07703		13. NUMBER OF PAGES 12 470
		15. SECURITY CLASS. (of this report) Unclassified
		15a. DECLASSIFICATION/DOWNGRADING SCHEDULE
16. DISTRIBUTION STATEMENT (of this Report) Approved for public release; distribution unlimited.		
17. DISTRIBUTION STATEMENT (of the abstract entered in Block 20, if different from Report)		
18. SUPPLEMENTARY NOTES To be entered in Defense Documentation Center.		
19. KEY WORDS (Continue on reverse side if necessary and identify by block number) microwave communication digital communication phase shift keying angle modulation quadrature partial response		
20. ABSTRACT (Continue on reverse side if necessary and identify by block number) The Avantek DRBA radio was tested in back-to-back configuration and an actual link configuration to determine transfer parameters and to refine standard test techniques. The radio operates at a baseband rate of 12.5526 Mb/s (192 voice channels) in a 7 MHz bandwidth in the 8 GHz band. The modulation technique is quadrature phase partial response (QPR). BER vs RSL characteristics are displayed as the primary mode of equipment evaluation. Carrier-to-interference data and diversity switching error data are presented. The power spectrum is		

OVER

TABLE OF CONTENTS

<u>PARAGRAPH</u>	<u>PAGE</u>
1. BACKGROUND	
1.1 Introduction	1
1.2 Approach to the Task	1
1.3 General Test Objectives	2
1.4 Summary of Results and Conclusions	2
1.5 Recommendations	2
2. GENERAL	
2.1 Description of Equipment	2
2.2 Methodology	5
2.3 Limitations	5
3. DETAILS OF TESTS	
3.1 Bit Error Rate vs Received Signal Level	6
3.2 Active Link Bit Error Rate Performance	10
3.3 Output Power	10
3.4 Carrier-to-Interference	12
3.5 Power Spectrum	20
3.6 Switching Errors	23
<u>APPENDICES</u>	
A. Simplified Map: CTA to Site Sibyl Microwave Link .	26
B. FCC Docket 19311 Abstract	27
C. Error Distribution Analysis	28

TABLE OF CONTENTS (cont)

<u>APPENDICES</u>	<u>PAGE</u>
D. Photograph of DR&A	34
E. Quadrature Partial Response Theoretical Curve . .	35
F. Digital Transmission Evaluation Project Reports .	40

LIST OF ILLUSTRATIONS

<u>FIGURE</u>	<u>PAGE</u>
1. DR8A System	4
2. Bit Error Rate vs Received Signal Level Test Configuration	7
3. Bit Error Rate vs Received Signal Level Range	9
4. Bit Error Rate vs Unavailability for Faded Link	11
5. Bit Error Rate vs Received Signal Level for Varying Output	13
6. Carrier-to-Interference Test Configuration	15
7. C/I Characteristic Curves (best performance)	16
8. C/I Characteristic Curves (worst performance)	17
9. C/I Comparison of Worst to Best Performance	18
10. C/I at Higher RSL's	19
11. Power Spectrum Test Configuration.	21
12. Power Spectrum with FCC Mask	22
13. Switching Error Test Configuration	24
14. Simplified Map: CTA to Site Sibyl Microwave Link.	26
15. Statistical Sample Size Relationships	32
16. Photograph of DR8A	34
17. Quadrature Partial Response Theoretical Curve BER vs S/N	38
18. Quadrature Partial Response Theoretical Curve BER vs Eb/No	39

1. BACKGROUND.

1.1 Introduction.

1.1.1 This document reports the results of tests performed on production engineering models of the Avantek DR8A digital microwave radio in back-to-back and active link configurations. This equipment was tested as part of the US Army Communications Command (USACC) Digital Transmission Evaluation Project (DTEP) during the period of May 1975 through February 1977.

1.1.2 By Department of the Army tasking, USACC issued Communications-Electronics Mission Order B74FUS136 in October 1973 to initiate the DTEP. This project contributes to the Army's efforts in the area of commercial development evaluations under DCA Circular 330-195-2.

1.1.3 The US Army Communications Systems Agency (USACSA), Fort Monmouth, New Jersey, is responsible for managing the DTEP. Actual conduct of the tests was delegated to the US Army Electronic Proving Ground (USAEPG), Fort Huachuca, Arizona, under the technical guidance and supervision of the US Army Communications-Electronics Engineering Installation Agency (USACEEIA), Fort Huachuca, Arizona.

1.2 Approach to the Task.

1.2.1 The tasking documents for the DTEP established several broad functions of equipment testing to be investigated and determined:

- a. Interface parameters between items of equipment.
- b. Transfer parameters within the system.
- c. Propagation path influences on transfer parameters.
- d. Test techniques and methodology.

1.2.2 To facilitate testing and limit variables, evaluations were scheduled in two phases. The first phase, known as the back-to-back tests, consisted of a series of tests with the equipment in a common location connected by waveguide and cabling. This configuration allowed accurate baseline parameters, test techniques, and performance tests, which could not be conducted on an active link with the desired degree of confidence.

1.2.3 The second phase of evaluations was performed on an active link from the Communications Test Area (CTA), Fort Huachuca to a repeater site (Site Sibyl) located in Texas Canyon near Benson, Arizona, a distance of approximately 32 miles (51 kilometers). A simplified map is provided in Appendix A.

1.3 General Test Objectives.

1.3.1 The purpose of the tests of the FR8A radio is to establish a data base and performance curves for comparison to performance curves of similar radios and to theoretical limits. Bit error rate (BER) curves describe overall performance at threshold and under various conditions of interference at various received signal levels (RSL's). The power spectrum is studied for out-of-band emissions and 99% power bandwidth. Errors in the mission bit stream caused by diversity switching are evaluated.

1.4 Summary of Results and Conclusions. Bit error rate at threshold showed a performance variance among radio combinations of approximately 3.5 dB, with the mean curve displaced about 4 dB from the theoretical maximum performance. The best performing combination was displaced 2.5 dB from theoretical, at a BER of 1×10^{-7} . Link testing showed virtually error free operation. Power output of up to 5 watts was realized without significant performance degradation. The C/I tests resulted in slightly degraded performance for ratios of 27 dB and 24 dB. Significant divergence in operating curves occurred for ratios of 21 dB and 18 dB with BER "plateaus" occurring at 2×10^{-6} and 2×10^{-4} , respectively. The 99% power bandwidth was 6 MHz. The transmitted spectrum met the 7 MHz FCC mask, assuming that the apparent noncompliance at -80 dBm is due to test equipment limitations. The radio was similarly compliant to the 6.3 MHz mask, with the exception of the orderwire transmission, which was significantly noncompliant. The receiver diversity switch performed error free, after alignment was completed.

1.5 Recommendations. Although limited reliability was encountered in some components of the engineering models which were tested, the Quadrature Phase Partial Response (QPR) modulation scheme employed provides 2 bps/Hz bandwidth utilization. This type of equipment is therefore recommended for DCS applications provided adequate reliability is demonstrated.

2. GENERAL.

2.1 Description of Equipment.

2.1.1 The DR8A radio, manufactured by Avantek, Inc., uses QPR modulation to increase transmitted bandwidth efficiency with a high ratio of input

bits transmitted to hertz of RF spectrum. QPR is a composite modulation technique employing four phase states and three amplitude levels. The emitted bandwidth of the DRBA is approximately 7 MHz and the input mission bit stream is a serial nonreturn to zero (NRZ) input of 12.5526 Mb/s, yielding an effective bandwidth efficiency of approximately 2 bits per second per hertz (bps/Hz). The mission bit stream of 12.5526 Mb/s is comprised of eight T1 lines at 1.544 Mb/s each, making available 192 voice channels. The radio consists of two transmitters providing for hot standby operation, and two receivers providing for space diversity reception. The radio also may be configured as a baseband repeater station by utilization of built-in strapping features. Figure 1 is a block diagram of the radio's major components.

2.1.2 Both the input and the output of the radio are wired through the control and alarm assembly. The control and alarm assembly interfaces with the encoder of each transmitter, where the input is split into two synchronized parallel bit streams of 6.276 Mb/s each, and then output to the QPR modulator. The input to this modulator uses filters having a cut-off frequency of approximately 3.1 MHz which provide a three-level partial response format to the linear biphase modulators. The outputs of the biphase modulators are combined in quadrature to provide the IF signal, which is now in a QPR format. The QPR IF signal then is up-converted to the carrier frequency and amplified by a traveling wave tube amplifier (TWT), operated at a low power level to insure linear performance. The output of the TWT is interfaced with the RF switch, where one signal is terminated and the other is directed to the diplexer for transmission.

2.1.3 The receiver operation is essentially the reverse of the transmitter's. The two receivers are identical, except for inclusion of a bandpass filter in the B receiver down converter. Since the B receiver is the space diversity receiver, it does not share an antenna with a transmitter and the signal does not pass through a diplexer. Therefore, a bandpass filter is provided to reject transmitter power received from the nearby primary antenna. Both receivers have greater than 70 dB rejection of the proximal transmitter's output. The down converter output is a 70 MHz IF which is filtered and amplified, and directed to the demodulator. The demodulator provides two outputs to the data recovery module, which are the I and Q channels. The data recovery module uses separate decision circuits to produce two parallel binary outputs (I and Q), which are combined into a single serial 12.5526 Mb/s stream. The 12.5526 Mb/s bit stream is then decoded, and fed to the control and alarm assembly.

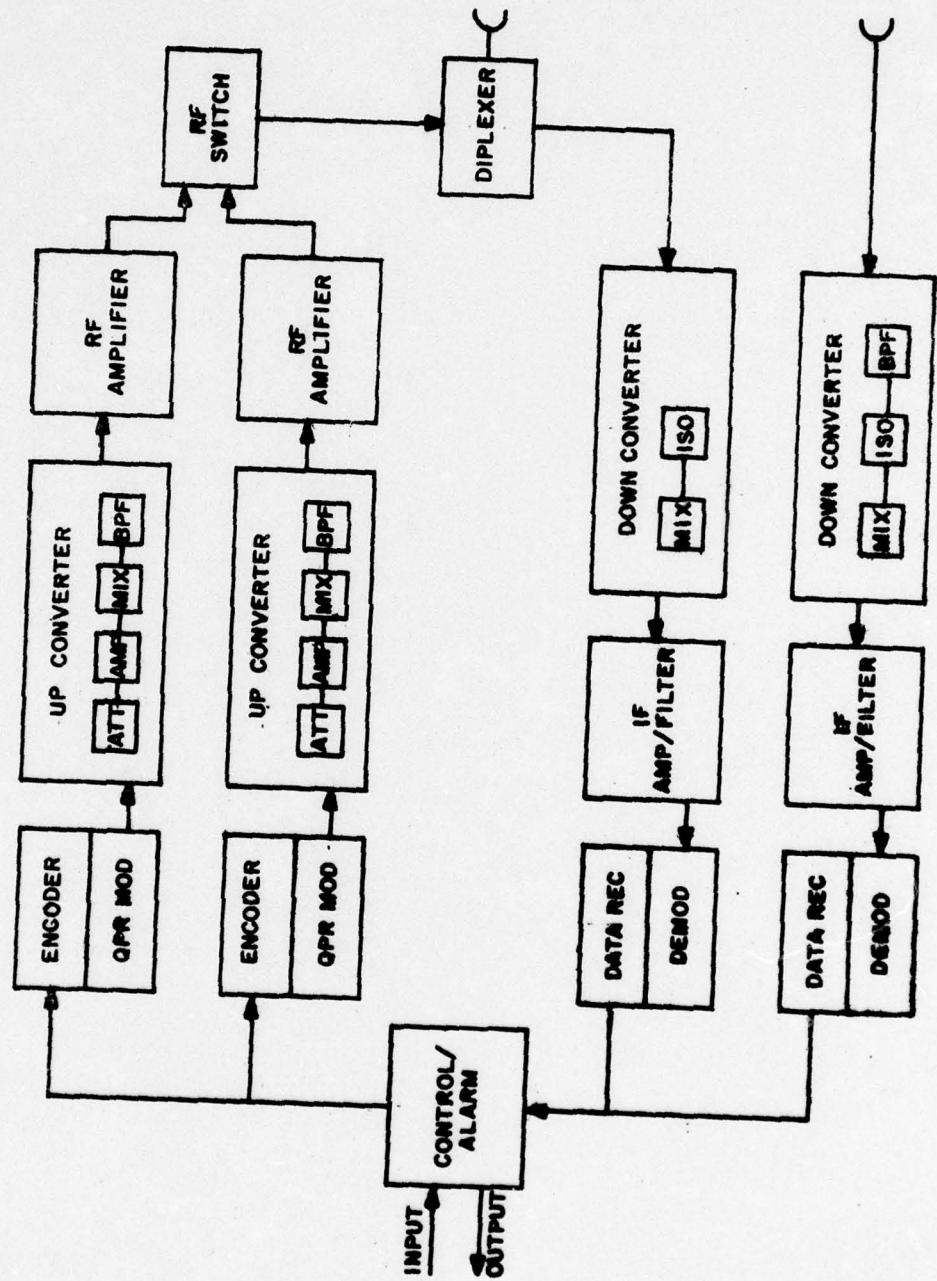


FIGURE 1. DRBA System

2.1.4 The control and alarm assembly contains the diversity switch, which selects the receiver output to be connected to the multiplexer. The diversity switch may be set for preference to either A, B, or to no preference, and contains time and phase delay equalization circuitry. The diversity switch is aligned with built-in incremental phase delay of 0 - 360 degrees by appropriately setting a series of six switches.

2.1.5 The DR8A uses a service channel to carry voice orderwire and alarms. The service channel has a maximum bandwidth of 50 KHz, and amplitude modulates an in-band auxiliary carrier located 3.45 MHz above the QPR carrier center frequency. The service channel carrier is combined with the QPR carrier prior to upconversion.

2.2 Methodology.

2.2.1 The procedures in testing this equipment followed standard practice, where established¹, as in noise figure and power output measurements.

2.2.2 Where procedures are established, but vary in details, as in BER measurements, the measurement time and number of data points recorded were adjusted to maximize confidence in the results.

2.2.3 Where exact procedures have not been standardized, various methods were tested with the final procedure being based on the validity of the results after analyzing the data.

2.2.4 Unless otherwise noted, all RSL's recorded were measured at the waveguide flange at the rack.

2.2.5 All BER measurements employed a pseudo-random pattern in excess of 32,000 bits in length.

2.3 Limitations.

2.3.1 Upon completion of back-to-back testing in October 1975, link testing was initiated. In February 1976 link testing was interrupted due to maintenance problems. A data decoder, demodulator plug-in and two stable local oscillators (STALO's) were returned to the contractor for repair. In September 1976, DTEP personnel assembled and activated a working system after factory representatives failed to complete repair. The system lacked one transmitter due to a faulty STALO and

1. Technical Evaluation of Line of Site and Troposcatter Links, DCS Quality Assurance Program, DCAC 310-70-57, Supplement 1, October 1974

TWTA power supply. Tests of BER vs RSL in the back-to-back configuration were performed again to determine the effects of the major repair on system performance. The results of this test showed that the BER vs RSL performance, before and after repair, were within 1 dB of each other.

2.3.2 Additional testing of the diversity switch was also performed. The results of this test are discussed in section 3.6.

2.3.3 No other unusual limitations were encountered in this study. Limits on the data were established by accuracy, stability, and re-setability of the test equipment and all items were constantly monitored for correct calibration.²

3. DETAILS OF TESTS.

3.1 Bit Error Rate vs Received Signal Level.

3.1.1 Objective. The purpose of this test is to gather data for plotting bit error rate (BER) against various received signal levels (RSL's). These curves yield important information for use in evaluating digital equipment. Combined effects of thermal noise, inter-symbol interference, and bandwidth are apparent and analysis is facilitated. Overall receiver performance can be analyzed by comparing the data from this test with theoretical predictions.

3.1.2 Procedure.

3.1.2.1 Figure 2 depicts the test configuration for this test. Signal levels from rack one to rack two were artificially faded with a variable waveguide attenuator. When positioned in the internal test mode, the 15-stage scramble shift register clocked internally, provides a pseudo-random bit stream with a repetition period of 32,767 bits. Connections enabled full duplex operation.

3.1.2.2 A power meter was connected to the input of the receiver to measure the RSL. The waveguide between racks was calibrated using the power meter. Signals were varied from higher levels to lower levels, with six independent measurements taken at each RSL. Rack one and rack two, A and B radios were tested for a total of eight sets of transmitter-receiver combinations.

3.1.3 Results and Analysis.

2. Calibration Requirements for the Maintenance of Army Materials,
DA TB 43180, December 1975

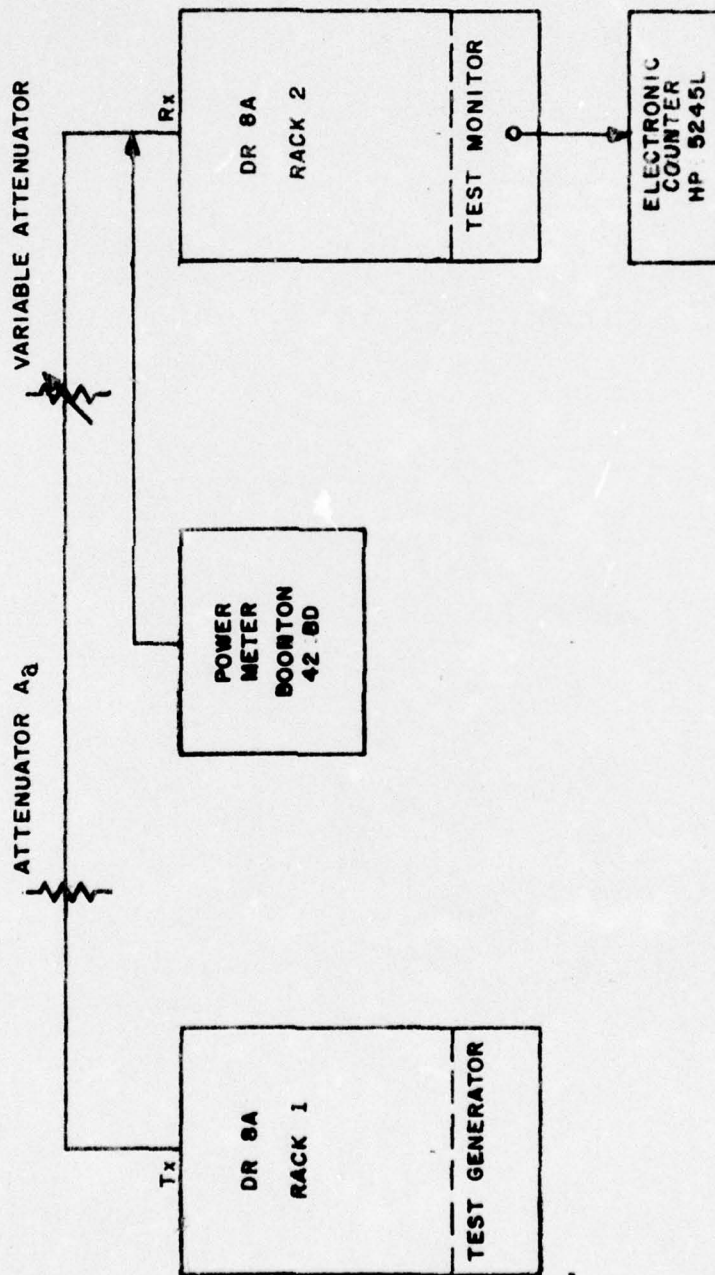


FIGURE 2. Bit Error Rate vs Received Signal Level Test Configuration

3.1.3.1 The range of performance is depicted in Figure 3. The two curves shown are the best performance combination and worst performance combination results with the remaining six curves evenly distributed in between. The worst case curve is displaced approximately 3.5 dB from the best case curve, which diverges from the theoretical QPR curve by approximately 2.5 dB at a BER of 1×10^{-7} .

3.1.3.2 Comparison of actual performance to theoretical limits is facilitated by correlating RSL to the ratio of energy-per-bit to noise power spectral density (E_b/N_0). Bit rate, bandwidth, and noise figure are consolidated in the resulting E_b/N_0 to RSL equation:

$$E_b/N_0 = (\text{RSL}) - (10 \log R + 10 \log kT + 30 + \text{NF})$$

Where RSL = received signal level in dBm

R = bit rate in bits-per-second

k = 1.38×10^{-23} joules per kelvin

T = 290 kelvin

30 = conversion factor from dBW to dBm

NF = receiver noise figure in dB

3.1.3.3 When the bit rate and bandwidth are identical, E_b/N_0 is equivalent to carrier-to-noise (C/N) ratio and to signal-to-noise (S/N) ratio. The modulation format used requires the coding of bits to symbols and so the E_b/N_0 values are not physically measurable. E_b/N_0 is, however, a convenient normalizing factor which allows comparison of modulation techniques and consolidates such variables as noise figure and bit per symbol coding.

3.1.3.4 The wider divergence from the theoretical as the RSL increases is an indication of the effects of the heavy filtering on the transmitted signal. At higher RSL's, the effects of intersymbol interference are more predominant, creating the divergence, while at the lower RSL's the effects of filtering are masked by the higher error rate due to noise.

3.1.3.5 The theoretical curve displayed in Figure 3 was derived from equations, which describe the probability of error as a function of

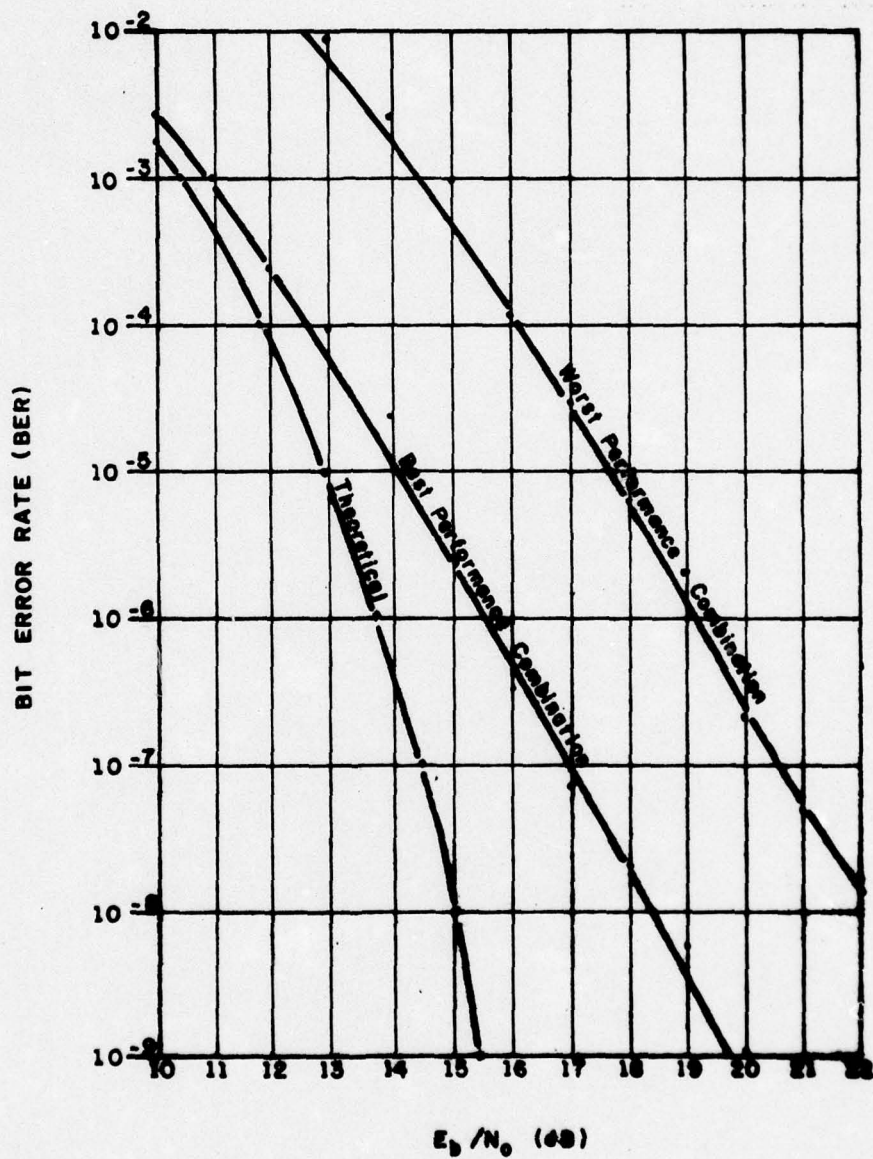


FIGURE 3. Bit Error Rate vs Received Signal Level Range

E_b/N_0 . This relationship is represented by:

$$P(e) = 9/4 \operatorname{erfc} \left\{ \pi/4 (E_b/N_0)^{1/2} \right\}$$

where $P(e)$ = probability of error
and erfc = the complementary error function

A full derivation of this relationship is given in Appendix E.

3.2 Active Link Bit Error Rate Performance.

3.2.1 Objective. The purpose of this test is to determine the link BER availability. That is, the percentage of time a specified BER performance level, or better, is available for system operation on an active microwave link.

3.2.2 Procedure. The test equipment and configuration are similar to that used in section 3.1 with the exception that the waveguide is replaced by an actual path. The CTA-Site Sibyl link was employed (Appendix A) with Site Sibyl as the transmitting site and errors recorded at CTA. The test was performed at normal link RSL (-35 dBm \pm 5 dB) with 240 second samples and at a faded link RSL (-71 dBm \pm 5 dB) with 30 second samples. The faded link RSL was obtained by attenuating the transmitted signal 35 dB with a variable waveguide attenuator.

3.2.3 Results and Analysis.

3.2.3.1 The results of the faded link testing are shown as unavailability (one minus availability) vs BER in Figure 4. A total of 27271 samples were taken with 66.2% (18050) error free. Of the remaining 9221 samples, 6922 contained less than 38 errors. Thus, 91.57% (24972) samples had a sample BER of 1×10^{-7} or better. The average BER was 4.18×10^{-8} . The worst BER was 3.457×10^{-6} .

3.2.3.2 For the unfaded link test 6670 samples were taken with 98.9% (6598) of the samples error free. All 6670 samples contained less than 40 errors or had a BER of 1.3×10^{-8} or better. The worst sample BER was 1.29×10^{-8} . The average BER was 2.1×10^{-11} .

3.3 Output Power.

3.3.1 Objective. The purpose of this test is to determine the effects of increased amplification of the output signal on the BER vs RSL performance.

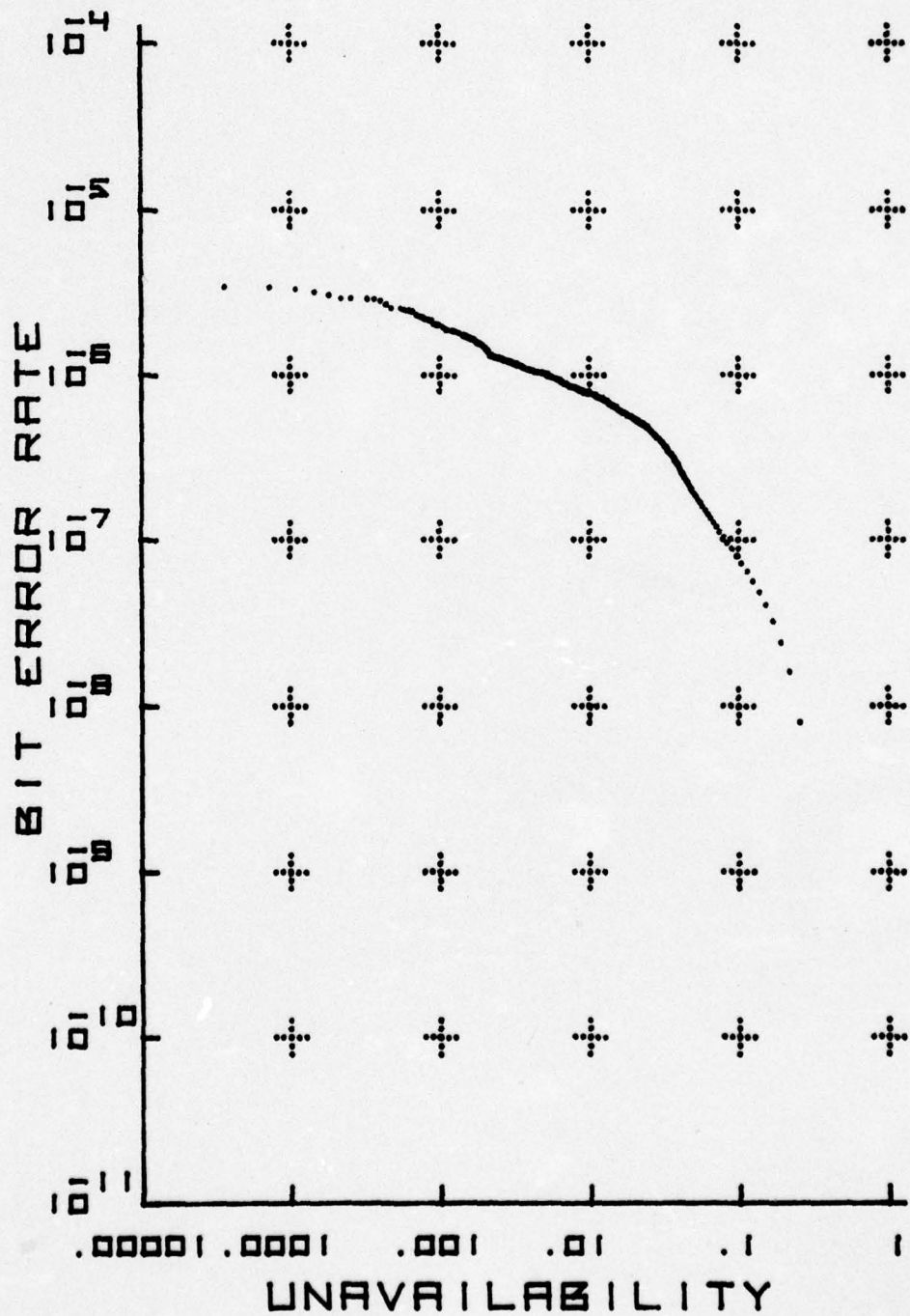


Figure 4. Bit Error Rate vs Unavailability for Faded Link

3.3.2 Procedure. The test configuration was the same as that for BER vs RSL section 3.1. The TWTA was adjusted for various output power levels between 2.5 watts and 10.0 watts. The signal level from rack one to rack two was artificially faded with a variable waveguide attenuator. A power meter was used to calibrate the waveguide run between racks.

3.3.3 Results and Analysis.

3.3.3.1 The radio system is designed with the TWTA constrained to operate in a linear region of its range. The maximum power output of the TWTA is much greater than the 2 watt nominal output. Linear amplification of the QPR signal is required because of the composition of the signal. Adjusting the TWTA for a higher power output causes the QPR signal to be distorted and increases BER.

3.3.3.2 Figure 5 depicts the performance degradation with increased amplification. The system operates up to 5.0 watts power output without significant degradation. However, above 5 watts the performance degradation is unacceptable.

3.4 Carrier-to-Interference.

3.4.1 Objective. The purpose of this test is to gather data in a controlled environment (back-to-back) for plotting BER against RSL for five ratios of added interference. These curves yield results necessary for the study of electromagnetic compatibility (EMC), isolation among systems in close geographic and spectral proximity, and isolation between orthogonal planes of polarization.

3.4.2 Procedure.

3.4.2.1 Cochannel, adjacent channel, and swept frequency interference tests were performed. Cochannel interference tests were performed on three receiver-transmitter combinations, based upon previous BER performance: best, worst, and median performance. Adjacent channel and swept frequency interference tests were performed on one combination, the set performing in the median range.

3.4.2.2 Calibration was conducted by setting the "RSL Attenuator" to zero and varying the "Interference Attenuator" to adjust the carrier-to-interference (C/I) level. A zero interference level was combined with a steady transmitter signal and the power was measured at the waveguide flange of the rack. Then the transmitter was disabled and the "Interference Attenuator" was adjusted for the appropriate power

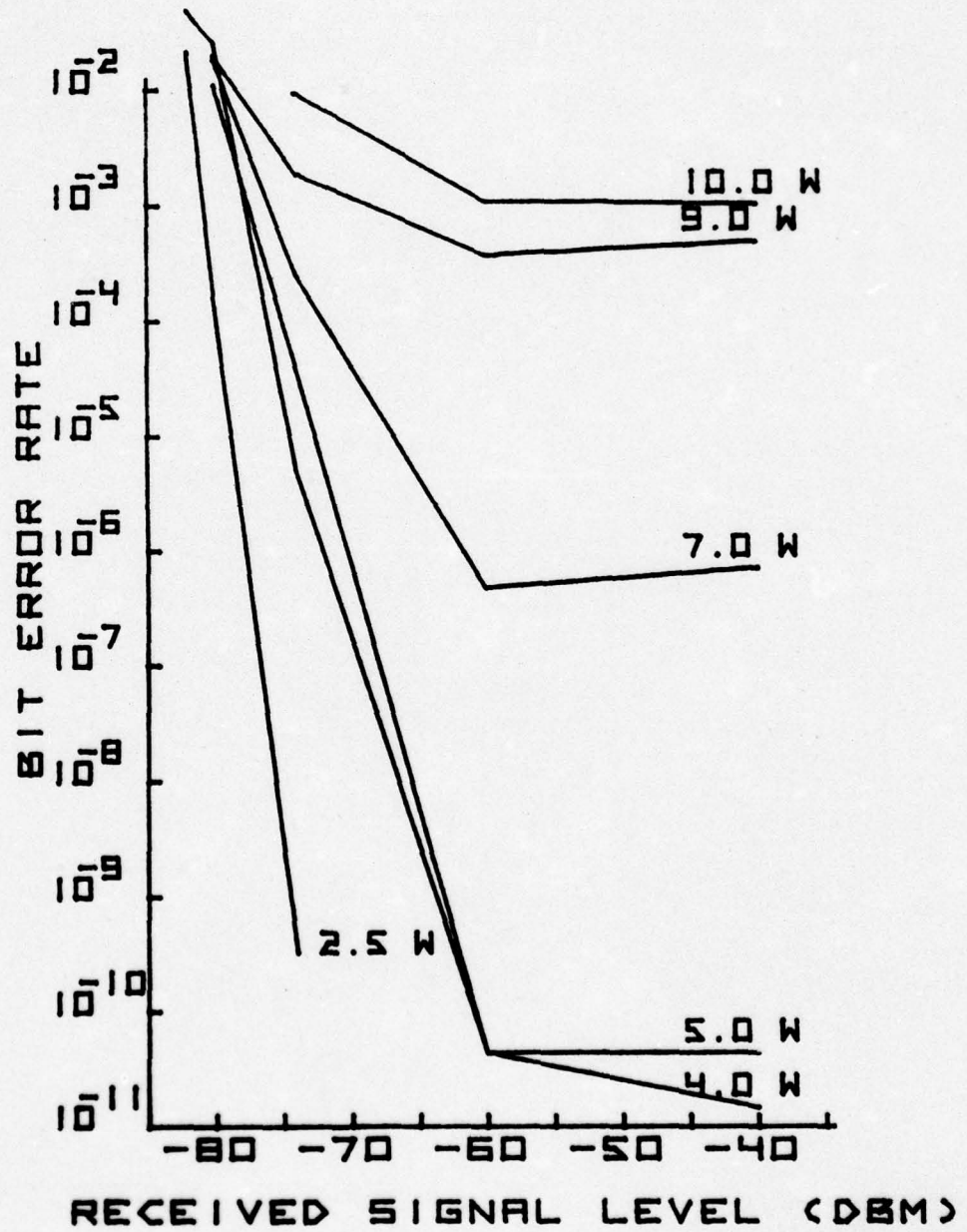


Figure 5. Bit Error Rate vs Received Signal Level for Varying Output

reading at the receiver for one C/I level. This completed the calibration and the test was conducted by varying only the "RSL Attenuator". The C/I remained constant for each measured RSL.

3.4.2.3 Tests of cochannel interference were made at C/I ratios of 12 dB, 15 dB, 18 dB, 21 dB, 24 dB, 27 dB, and with no interference. The interference oscillator was switched to CW mode and frequency was adjusted to the carrier frequency. Repeatability of the data was confirmed by five test runs.

3.4.2.4 The interference oscillator was set to triggered sweep mode for the swept frequency interference test. The frequency was varied up to ± 50 MHz from the carrier frequency. Tests were run for C/I ratios of 12 dB, 15 dB, 18 dB, 21 dB, 24 dB, 27 dB and no interference. Five tests at each ratio were accomplished.

3.4.2.5 The adjacent channel interference test was conducted with the AN/FRC-80(V) utilizing a three-level partial response modulation format as the interfering source. The carrier frequency of the AN/FRC-80(V) was 20 MHz above the carrier frequency of the DR8A. Tests were performed five times each with C/I ratios of 12 dB, 15 dB, 18 dB, 21 dB, 24 dB, 27 dB, and with no interference.

3.4.3 Results and Analysis.

3.4.3.1 Of the three types of interference tests performed, only the cochannel interference results are plotted. Figure 7 is the plot of the best performance radio combination while Figure 8 is the plot of the worst performance combination. Figure 8 is a comparison of the 15 dB, 24 dB, and no interference C/I ratios for the best performance combination and worst performance combination. As can be seen in Figure 9, the additional degradation in the worst case increased with higher interference levels. At a BER of 1×10^{-7} and a C/I ratio of 24 dB the required RSL was approximately -69 dBm. For C/I ratios of 18 dB and less, a BER of 1×10^{-7} was not achieved. The increased susceptibility of QPR modulation is demonstrated by comparing these results to those obtained for QPSK modulation as depicted in DTEP, RDS-80 Final Report (CCC-CED-75-DTEP-004). In addition, a C/I ratio of 12 dB proved to be too little, and the radio could not decode the signal satisfactorily.

3.4.3.2 Additional tests were performed at higher RSL's to determine if BER "plateaus" existed. Figure 10 depicts the results of these tests. The plots are for C/I ratios of 18 dB, 21 dB, and 24 dB

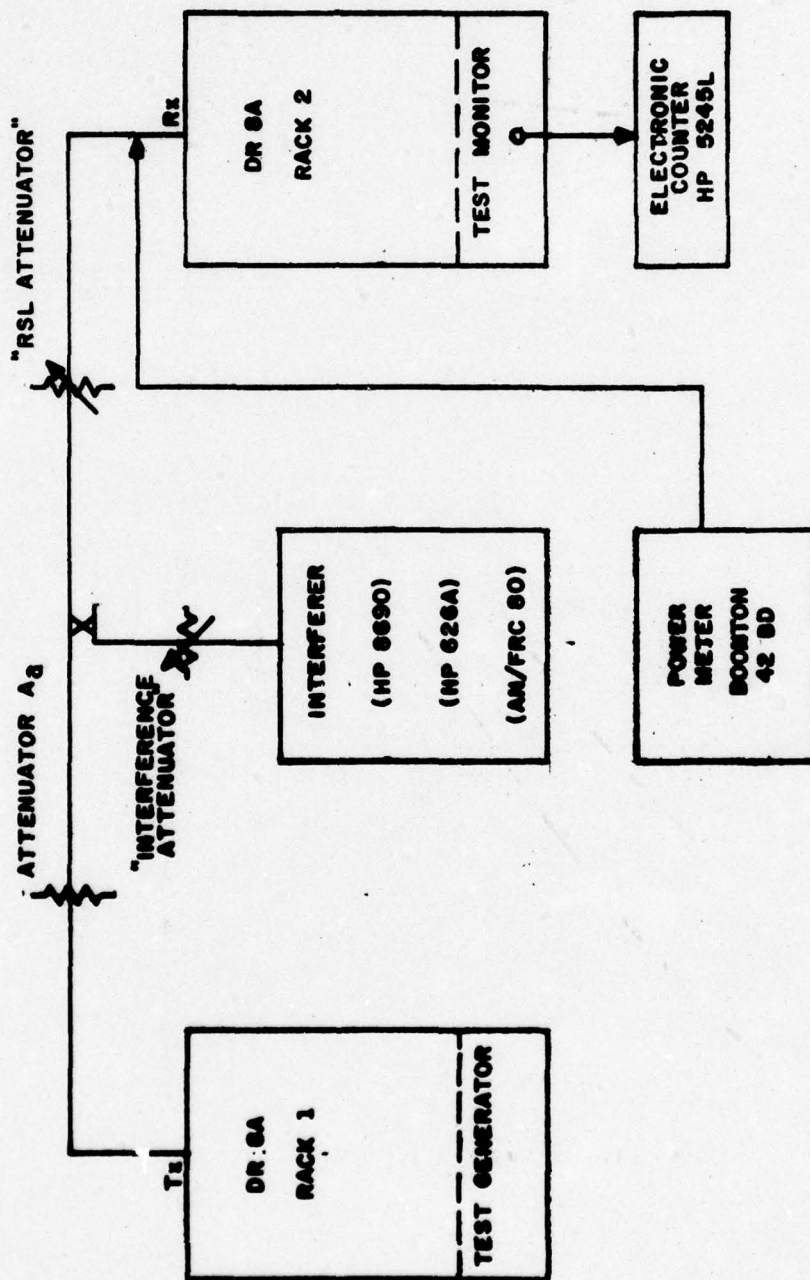


FIGURE 6. Carrier-to-Interference Test Configuration

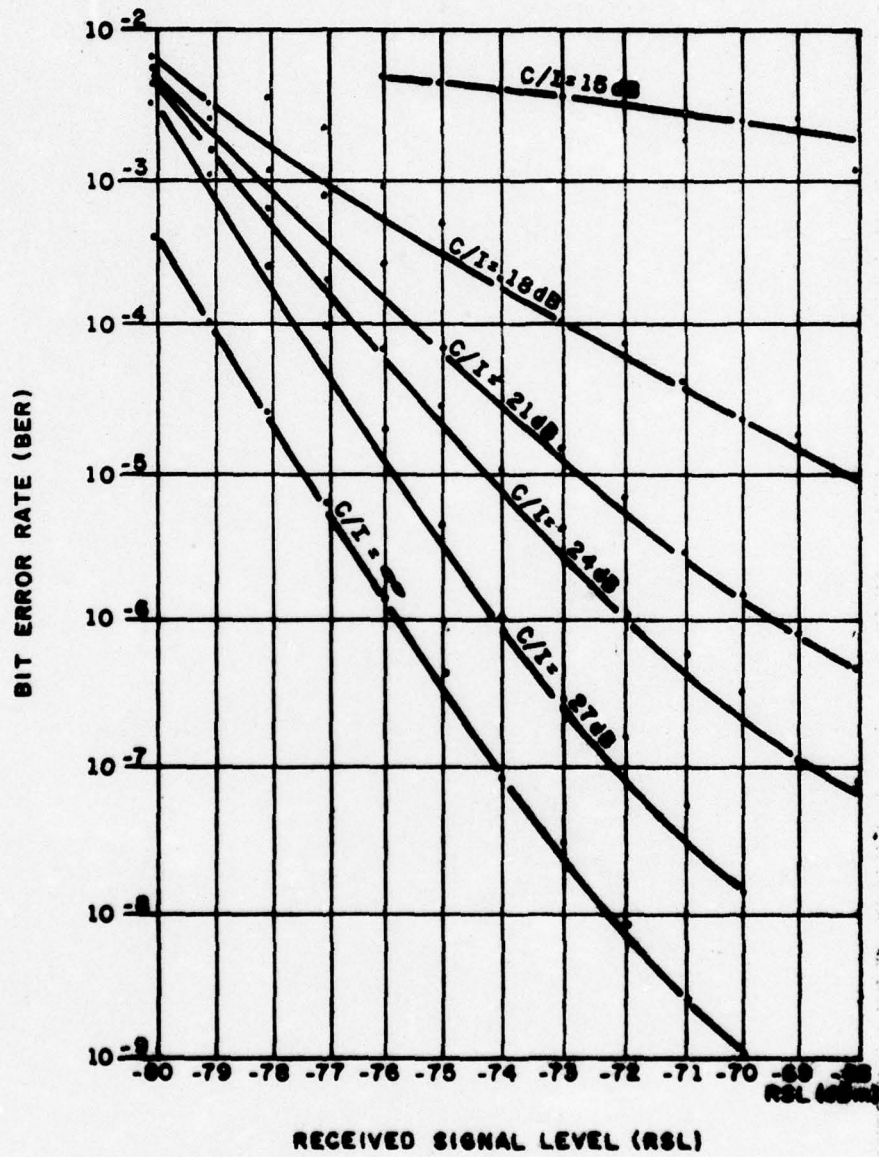


FIGURE 7. C/I Characteristic Curves (best performance)

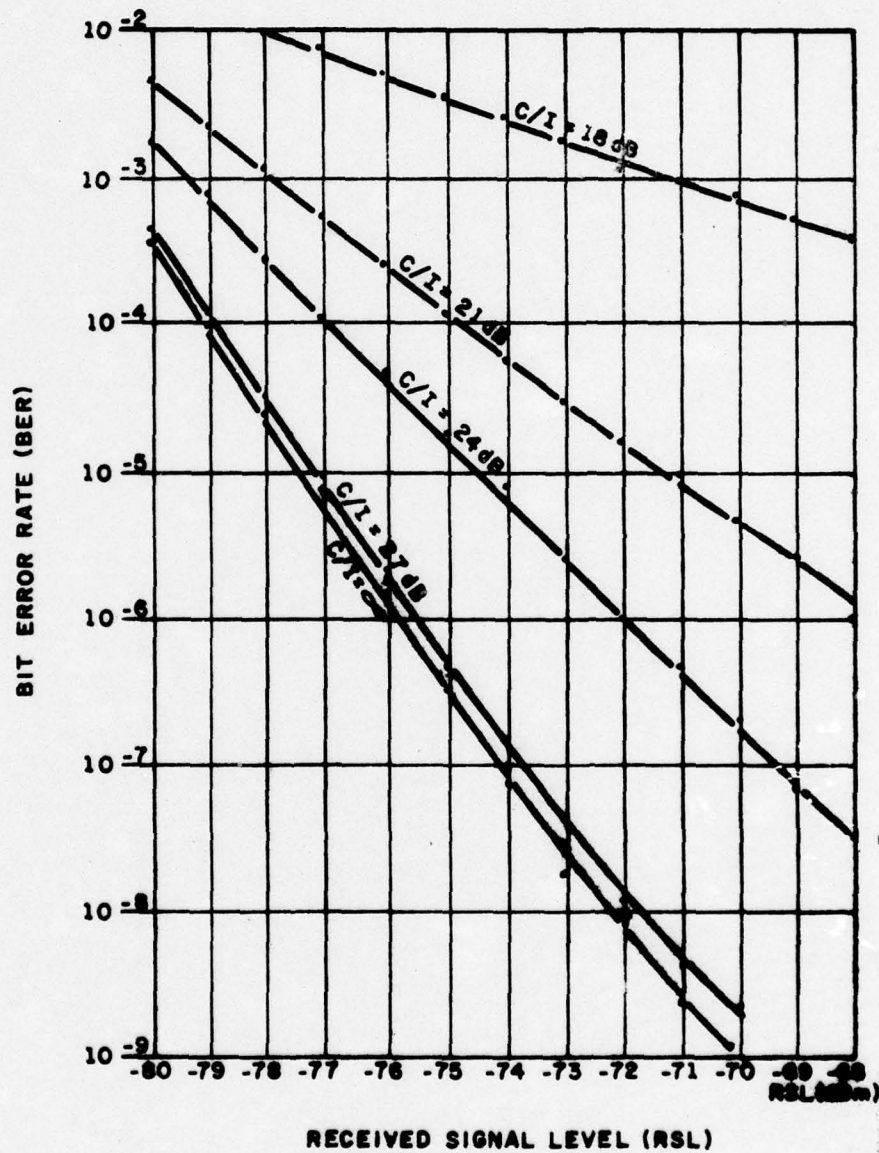


FIGURE 8. C/I Characteristic Curves (worst performance)

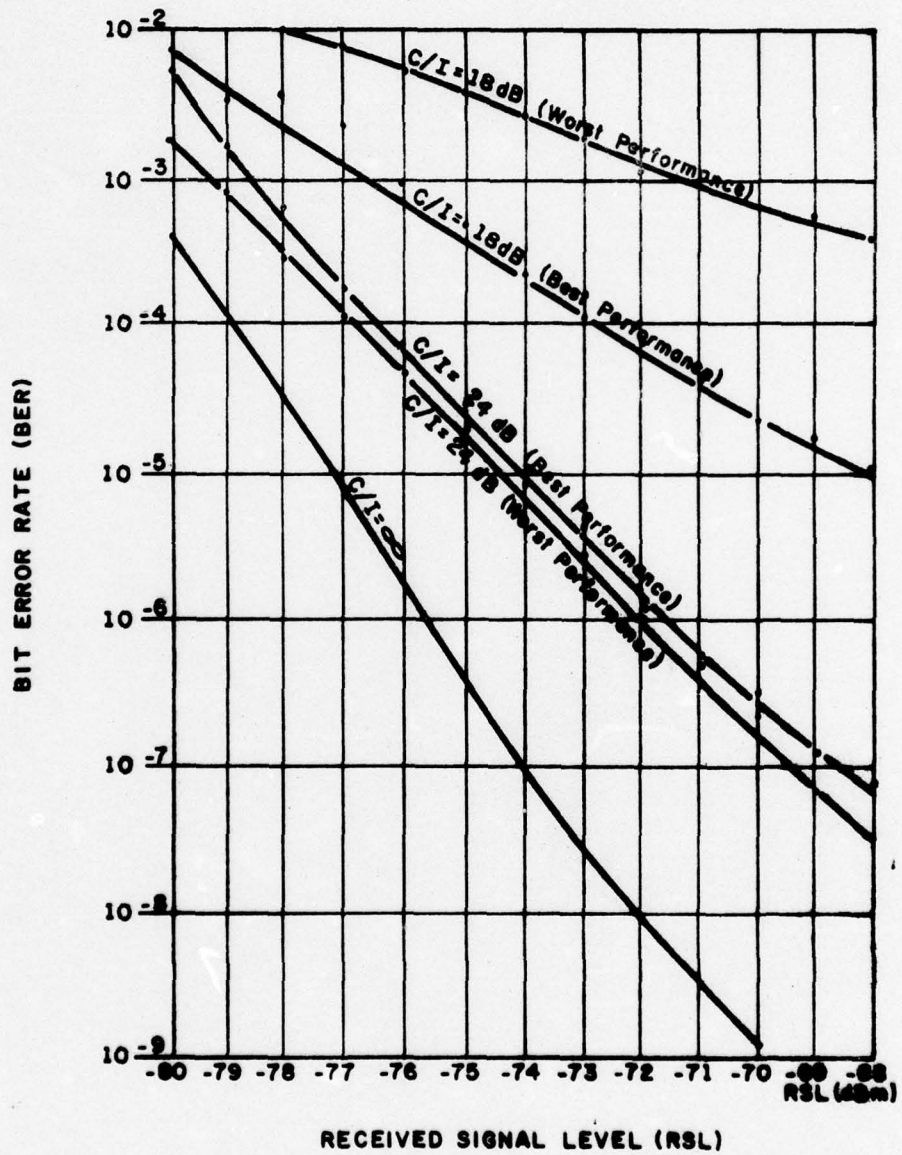


FIGURE 9. C/I Comparison of Worst to Best Performance

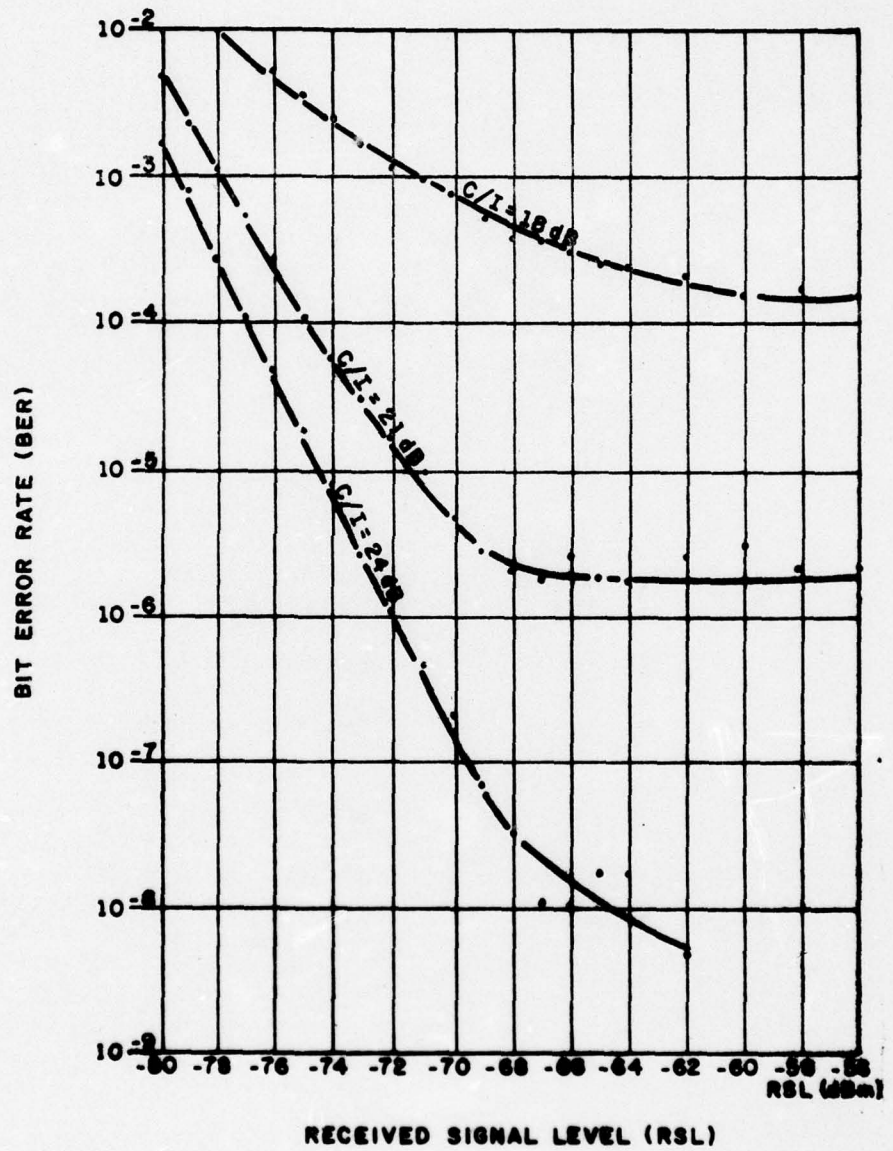


FIGURE 10. C/I at Higher RSL's

are best performance combinations results. The 18 dB C/I ratio curve forms a plateau at a BER of approximately 2×10^{-4} and the 21 dB C/I ratio curve has a plateau at a BER of approximately 2×10^{-6} .

3.4.3.3 The results of the swept frequency and adjacent channel interference are not plotted, as they had a negligible effect on the radio's performance.

3.5 Power Spectrum.

3.5.1 Objective. The purpose of this test is to provide data on equipment power spectral density curves. Rejection of out-of-band emissions to the level required by FCC Docket 19311 and 99% power bandwidth are analyzed.

3.5.2 Procedure.

3.5.2.1 The equipment configuration for plotting spectral power density curves is shown in Figure 11. A small amount of power was taken from the directional coupler in the waveguide and displayed on a Hewlett-Packard 141T spectrum analyzer with appropriate plug-in units. A hard copy of the spectrum was obtained by using an X-Y plotter driven by appropriate sources within the analyzer display unit.

3.5.2.2 In order to reference the displayed spectrum accurately to the appropriate FCC Docket 19311 requirements, total radiated power measurements of both modulated and unmodulated carriers were also made employing a Boonton 42 BD power meter and a 41-4D power sensor.

3.5.3 Results and Analysis.

3.5.3.1 The spectra for each transmitter were similar and the spectrum displayed in Figure 12 is typical. The 99% power bandwidth was approximately 6 MHz. The 8.5 MHz mask, illustrated in Figure 10 is applied to show the degree of compliance with Docket 19311 limitations. When the formula for calculating necessary bandwidth in the Docket Abstract (Appendix B) is used, there appears to be noncompliance beyond $f_0 \pm 8$ MHz. However, due to ambient noise level limitations, the spectrum analyzer's range is limited to approximately 48 dB. Therefore, the amount of compliance at -50 dB cannot be proved, but can be assumed based on the spectrum roll-off.

3.5.3.2 The 7 MHz mask was applied to study conformance to the stated bandwidth of the equipment. As can be seen, marginal noncompliance is observed beyond $f_0 \pm 6.5$ MHz, where analyzer noise is a limitation.

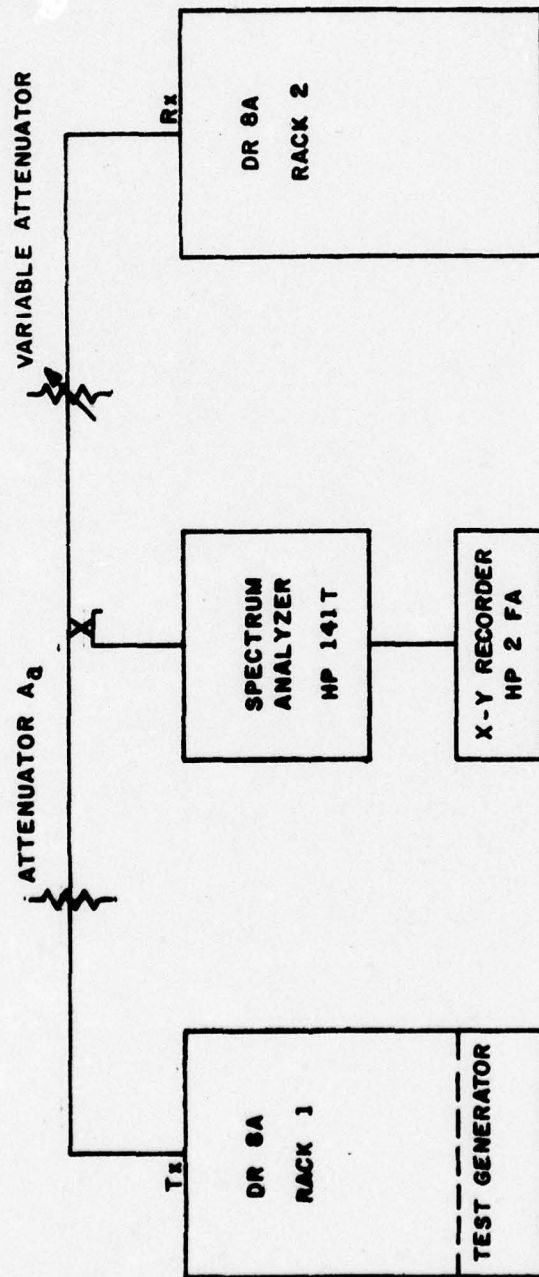


FIGURE 11. Power Spectrum Test Configuration

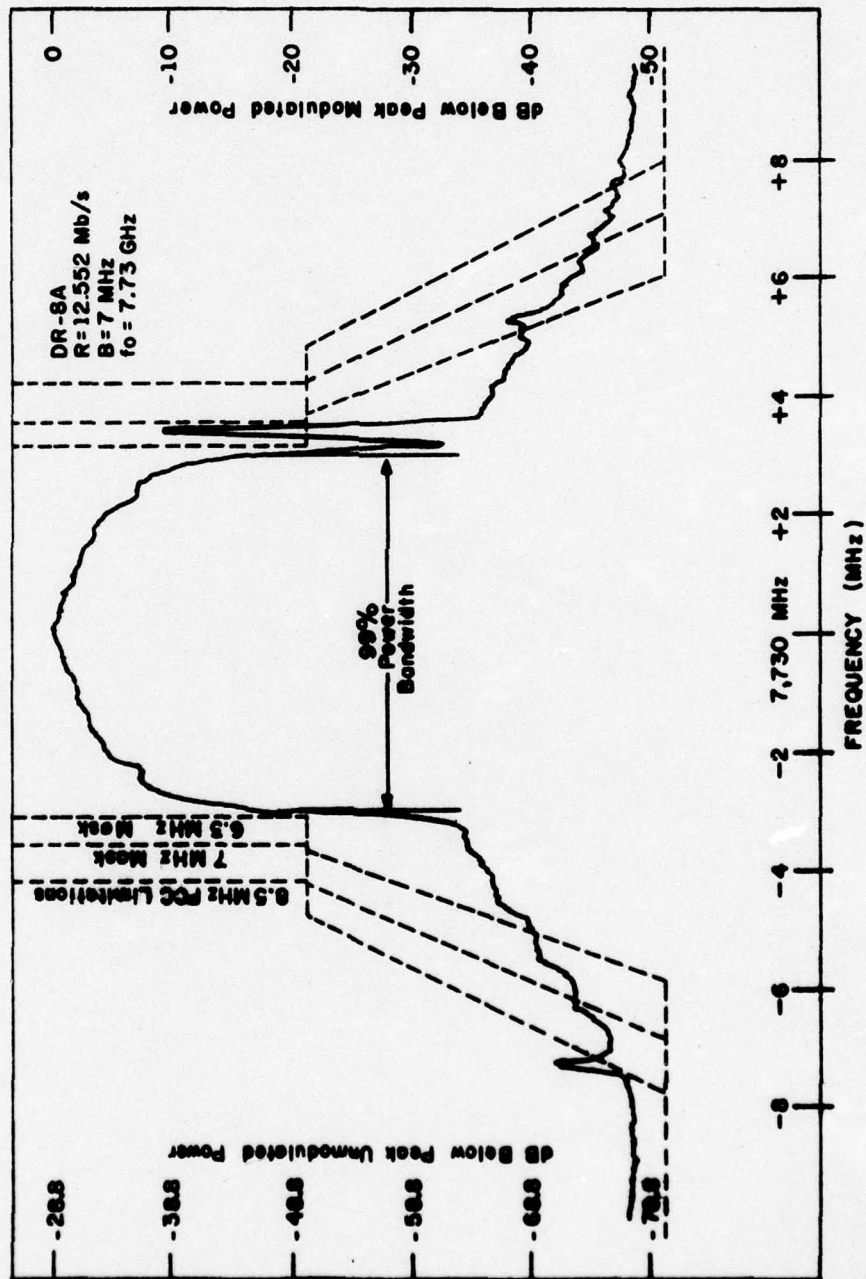


Figure 12. Power Spectrum with FCC Mask

The 6.3 MHz mask is applied to show the conformance necessary for exactly 2 bps/Hz operation. Noncompliance occurs at $f_0 \pm 3.5$ MHz, where the service channel is operating, and beyond approximately $f_0 \pm 5.0$ MHz, where the attenuation is deficient by as much as 10 dB.

3.6 Switching Errors.

3.6.1 Objective. The purpose of this test is to measure errors generated when switching receivers both manually and automatically. When the diversity switch is aligned properly, the receiver should operate without error.

3.6.2 Procedure.

3.6.2.1 The equipment configuration for this test was the same as that used for BER vs RSL. The digital logic switch controls were activated by remotely controlled command, waveguide fading, and manual switching.

3.6.2.2 The initial testing was performed with the diversity switch correctly aligned to compensate for internal time and phase delays of the radio. A second test was performed with adverse delay times of 8 and 15 nanoseconds introduced to the system. A third test was performed with increased phase delays of 0, ± 30 and ± 60 degrees, which are analogous to time delays of 0, ± 13 and ± 27 nanoseconds, induced in the system. Ten switching actions were accomplished for each method for each test.

3.6.2.3 Further examination of time delays between receivers was performed after repair of equipment. The equipment configuration was the same. The transmitter was switched from A transmitter to B transmitter and back 58 times and the time differential between the receivers was recorded.

3.6.3 Results and Analysis.

3.6.3.1 With the diversity switch properly aligned, error free operation was observed when switching was induced by all three methods.

3.6.3.2 For testing performed with the induced time delays of 8 and 15 nanoseconds, no errors were recorded. No errors were recorded for testing performed with the induced phase delay for 0, ± 30 , and ± 60 degrees. With -60 degree phase delay and manual switching one of ten switching operations from A receiver to B receiver had an error occurrence of 28 errors, and two of ten switches from B to A had error occurrences of 25 and 58 errors. With -60 degree phase delay and remote switching from receiver B to A there were two of ten transfers with error

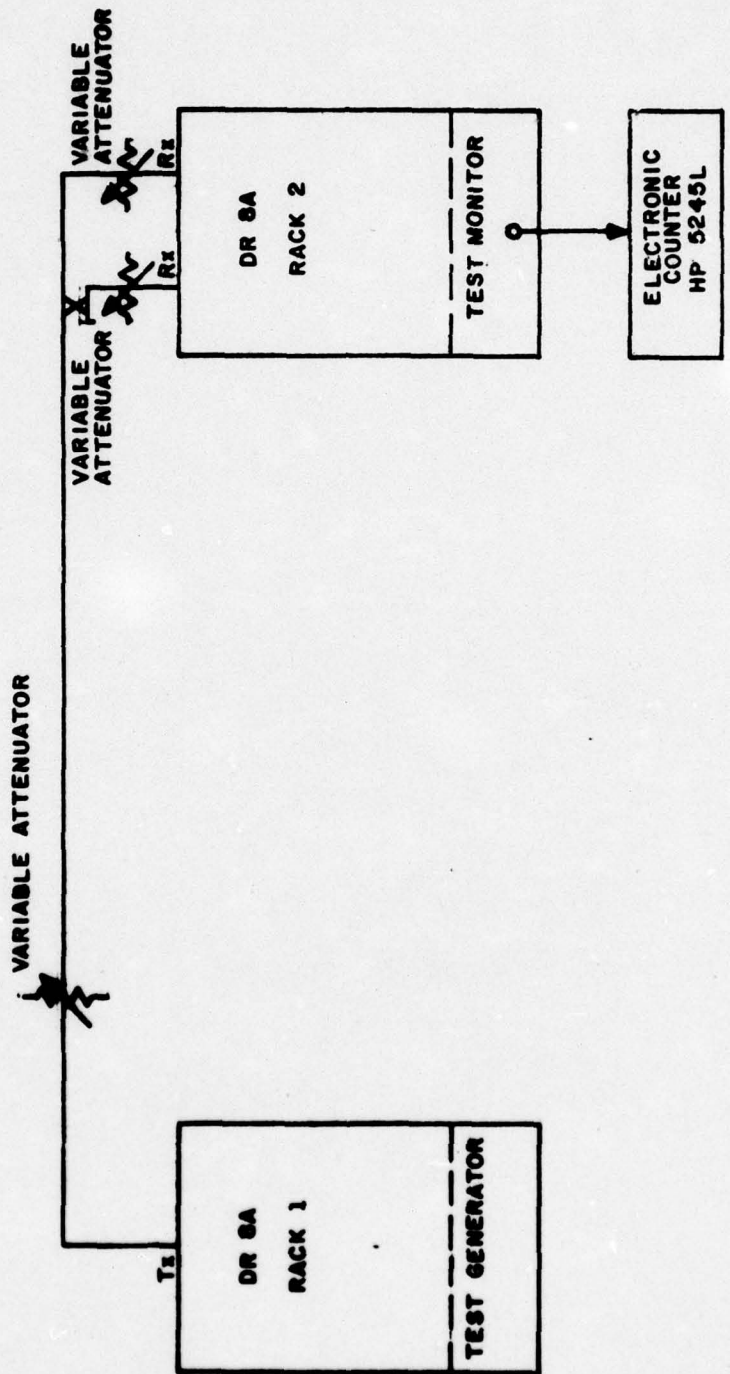


FIGURE 13. Switching Error Test Configuration

Occurrences of 34 and 98 errors; from receiver A to B there were two of ten switches with error occurrences of 45 and 90 errors. All others were error free and no multiplexer reframes occurred.

3.6.3.3 When a transmitter switch occurred during initial switch testing, a change in the relative time delay between receivers also occurred. Additional investigation of this change showed four possible relationships between the A and B receivers. The time differential at the input to the diversity switch was 5, 10, 15, or 20 nanoseconds, with a majority (39%) of the transmitter switches causing the 20 nanosecond state and 31% being the 15 nanosecond state. It should be noted that the possible change in the delay of B relative to A is equivalent to the largest amount of differential delay the Vicom T1-4000 multiplexer will accept. Thus the diversity switch alignment is critical to system performance.

APPENDIX A

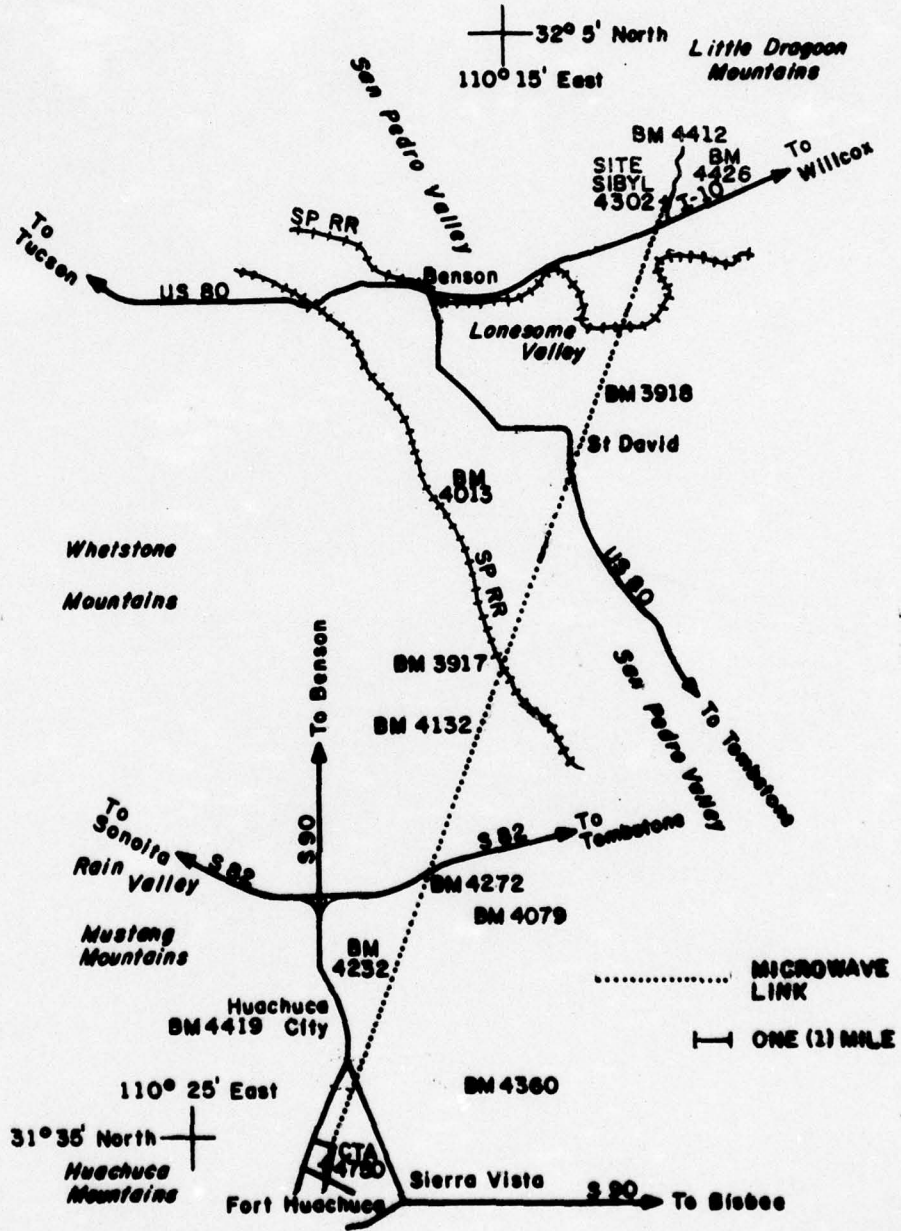


Figure 14. Simplified Map: CTA to Site Sibyl Microwave Link

APPENDIX B
FCC DOCKET 19311 ABSTRACT

FCC Docket Number 19311 was formally released on 27 September 1974 to be effective 1 November 1974. Pertinent points of this docket with respect to this report are the determination of necessary bandwidth and the emission limitations restriction. The determination of the necessary bandwidth of digital modulation using PSK (F9Y) is given by the formula $B_n = \frac{2RK}{\log_2(S)}$

Where: B_n = necessary bandwidth in MHz
R = bit rate in bits-per-second
K = 1
S = number of signaling states

Substituting the values for 12.6 Mb/s data into a QPSK transmitter yields:

$$B_n = \frac{2 (12.6 \times 10^6) (1)}{\log_2(4)}$$
$$B_n = \frac{25.2 \times 10^6}{2} = 12.6 \text{ MHz}$$

This means that for a system employing QPSK modulation, the necessary bandwidth in hertz is numerically equal to the bit rate in bits-per-second.

For systems operating below 15 GHz, the radiated emissions must be contained within a "mask" comprised of several segments. Measurements to apply these segments are required to be made in 4 kHz band increments. The attenuation required below the mean power output is given by the formula:

$$A = 35 + 0.8 (P-50) + 10 \log_{10}(B)$$

Where: A = attenuation (in decibels) below the mean output power level
P = percent removed from the carrier frequency
B = authorized bandwidth in MHz

This must be tempered by two additional limitations. First, the attenuation greater than 50 percent removed must be a minimum of 50 dB, and secondly, attenuation greater than 80 dB is not required.

APPENDIX C

ERROR DISTRIBUTION ANALYSIS

In order to measure the bit error rate (BER) of a system, it is necessary to take samples of the bit stream and observe the number of errors that occur. The number of errors is then divided by the total number of bit times in the sample, and the resulting proportion is the average BER for the sample. (The total number of bit times in the sample is found by multiplying the system bit rate by the sample duration.)

Bit stream error rate measurements must include some indication of their significance or accuracy, in order to be meaningful. The significance of a BER measurement generally is expressed as a confidence level. For example, one might say that he is 99% confident that the average BER of a system is less than or equal to one error in 10^7 bits ($BER = 1 \times 10^{-7}$).

The level of confidence that may be assigned to any BER measurement is based upon some acquired or assumed knowledge of the statistical nature of errors in the bit stream. Detailed information on the statistical behavior of errors in a system is seldom available and may be difficult and costly to obtain. Therefore, errors generally are assumed to follow a binomial distribution. This assumption implies that the probability of an error in any single bit time is a constant, and is independent of whether an error occurred in any previous bit time. The probability that a particular number of errors will be observed in a sample is then given by:

$$P_x = \frac{n!}{x! (n-x)!} (BER)^x (1 - BER)^{(n-x)}$$

where: n = number of bit times in sample

x = number of errors in the sample

BER = actual bit error rate (probability of error)

With the occurrence of errors thus mathematically characterized, confidence limits for BER measurements may be established. The table in this appendix contains the required information.

In order to use the tabulated information, find the number of errors observed in the sample in the left-hand column under "c". Read across the row to the column for required confidence level. If a two-sided confidence interval is desired, note the values under both "L" and "U". If a one-sided confidence interval is desired, only the value under "U" need be noted. The values thus obtained are

L = factor for lower limit
 U = factor for upper limit

n = prescribed sample size
 c = observed number of errors ($\leq 0.1 n$)

		CONFIDENCE LEVEL							
1-sided	90%	95%		97.5%		99.5%			
2-sided	80%	90%		95%		99%			
	L	U	L	U	L	U	L	U	
0	.000	2.3	.000	3.0	.000	3.7	.000	5.3	
1	.105	3.9	.051	4.7	.025	5.6	.005	7.4	
2	.53	5.3	.36	6.3	.242	7.2	.103	9.3	
3	1.10	6.7	.82	7.8	.62	8.8	.34	11.0	
4	1.74	8.0	1.37	9.2	1.09	10.2	.67	12.6	
5	2.43	9.3	1.97	10.5	1.62	11.7	1.08	14.1	
6	3.15	10.5	2.61	11.8	2.20	13.1	1.54	15.7	
7	3.9	11.8	3.3	13.1	2.81	14.4	2.04	17.1	
8	4.7	13.0	4.0	14.4	3.5	15.8	2.57	18.6	
9	5.4	14.2	4.7	15.7	4.1	17.1	3.13	20.0	
10	6.2	15.4	5.4	17.0	4.8	18.4	3.7	21.4	
11	7.0	16.6	6.2	18.2	5.5	19.7	4.3	22.8	
12	7.8	17.8	6.9	19.4	6.2	21.0	4.9	24.1	
13	8.6	19.0	7.7	20.7	6.9	22.2	5.6	25.5	
14	9.5	20.1	8.5	21.9	7.7	23.5	6.2	26.8	
15	10.3	21.3	9.2	23.1	8.4	24.7	6.9	28.2	
16	11.1	22.5	10.0	24.3	9.1	26.0	7.6	29.5	
17	12.0	23.6	10.8	25.5	9.9	27.2	8.3	30.8	
18	12.8	24.8	11.6	26.7	10.7	28.4	8.9	32.1	
19	13.7	25.9	12.4	27.9	11.4	29.7	9.6	33.4	
20	14.5	27.0	13.3	29.0	12.2	31	10.4	35	

c	L	U	L	U	L	U	L	U
21	15.4	28.2	14.1	30.2	13.0	32	11.1	36
22	16.2	29.3	14.9	31.4	13.8	33	11.8	37
23	17.1	30.5	15.7	32.6	14.6	35	12.5	38
24	18.0	31.6	16.6	33.8	15.4	36	13.3	40
25	18.8	33	17.4	35	16.2	37	14.0	41
26	19.7	34	18.2	36	17.0	38	14.7	42
27	20.6	35	19.1	37	17.8	39	15.5	43
28	21.5	36	19.9	38	18.6	40	16.2	45
29	22.3	37	20.7	40	19.4	42	17.0	46
30	23.2	38	21.6	41	20.2	43	17.8	47
35	27.7	44	25.9	46	24.4	49	21.6	53
40	32.1	49	30.2	52	28.6	54	25.6	59
45	36.6	55	34.6	58	32.8	60	29.6	65
50	41.2	60	39.0	63	37.1	66	33.7	71
55	46	66	43	69	41	72	38	77
60	50	71	48	74	46	77	42	83
65	55	77	52	80	50	83	46	89
70	60	82	57	85	55	88	50	95
75	64	87	61	91	59	94	55	100
80	69	93	66	96	63	100	59	106
85	73	98	70	102	68	105	63	112
90	78	103	75	107	72	111	67	117
95	83	109	80	113	77	116	72	123
100	87	114	84	118	81	122	76	129

next converted to BER values using the formula:

$$\text{BER} = \frac{(\text{U or L})}{\text{sample size}}$$

These BER values are the desired confidence limits. For example, a 10 second sample is taken from a bit stream with rate 12.55 Mb/s and 15 errors are observed. The sample size is $n = 10 \times 12.55 \times 10^6 = 1.255 \times 10^8$ bits. From the table, with $c = 15$ corresponding to the number of errors observed, one sees that the 90% confidence limits (upper and lower) for the true BER are:

$$\frac{9.2}{1.255 \times 10^8} = 7.3 \times 10^{-8} \quad \text{and} \quad \frac{23.1}{1.255 \times 10^8} = 1.84 \times 10^{-7}$$

Alternatively, for one-sided confidence, it may be stated with 90% confidence, that the true bit error rate is less than or equal to:

$$\frac{21.3}{1.255 \times 10^8} = 1.70 \times 10^{-7}$$

Similarly, the 99% confidence limits (upper and lower) for the true BER are:

$$\frac{6.9}{1.255 \times 10^8} = 5.5 \times 10^{-8} \quad \text{and} \quad \frac{28.2}{1.255 \times 10^8} = 2.25 \times 10^{-7}$$

Or, we may state with 99.5% confidence (one sided) that the true BER is less than or equal to:

$$\frac{28.2}{1.255 \times 10^8} = 2.25 \times 10^{-7}$$

Of course, the width of the confidence interval is reduced as the sample size is increased. For example; if the bit stream of the previous example had been sampled for 50 seconds and 75 errors were observed, the 90% confidence limits (upper and lower) for the true BER would have been:

$$\frac{61}{50 \times 12.55 \times 10^6} = 9.7 \times 10^{-8} \quad \text{and} \quad \frac{91}{50 \times 12.55 \times 10^6} = 1.45 \times 10^{-7}$$

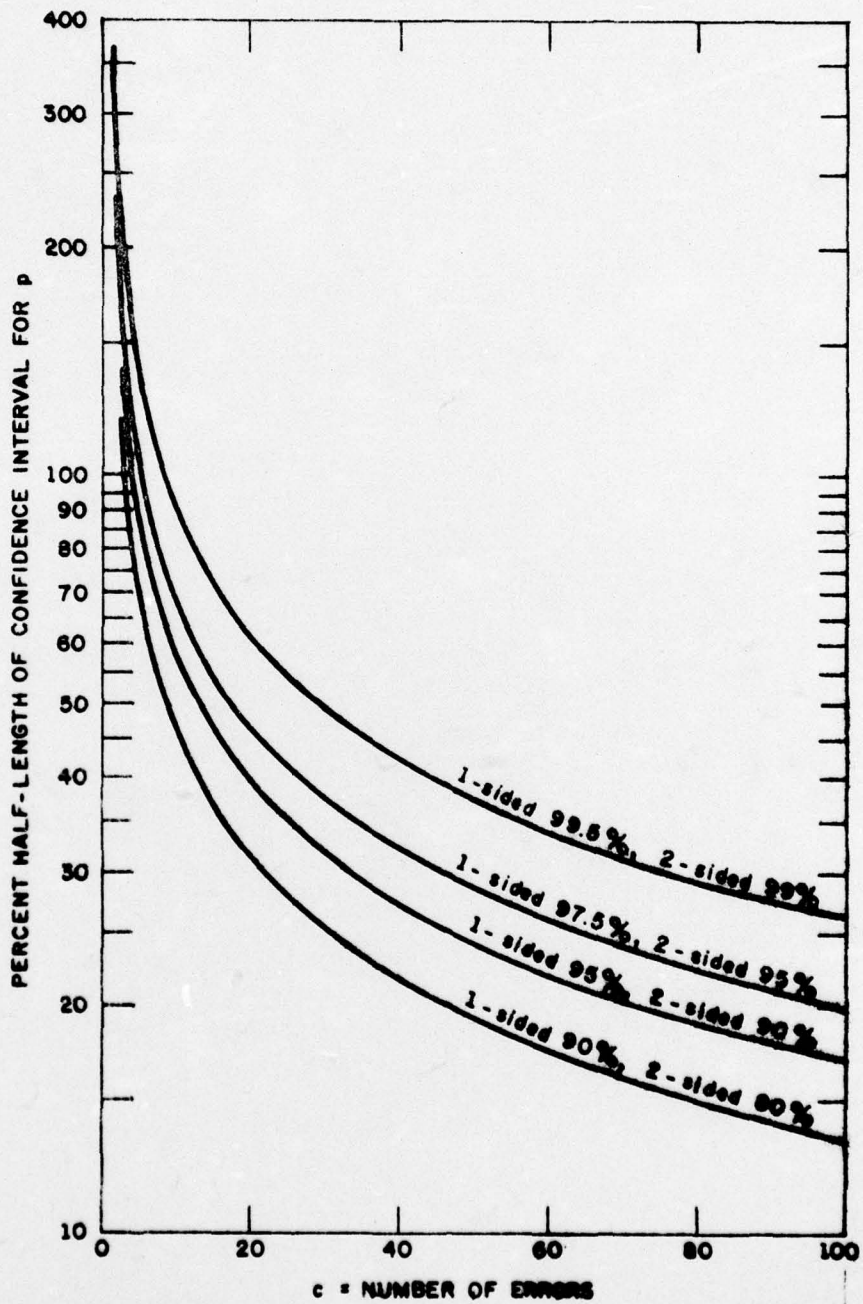


Figure 15. Statistical Sample Size Relationships

Or, it could have been stated with 90% confidence (one-sided) that the true BER was less than or equal to:

$$\frac{66}{50 \times 12.55 \times 10^6} = 1.05 \times 10^{-7}$$

If some estimate of the true BER of a system is available before a measurement is to be taken, a reasonable approximation of the sample size required for any desired accuracy and confidence level may be determined.

For example: The BER of a system under test is estimated as 1 error in 10^6 bit times (BER = 1×10^{-6}). A determination of testing sample size is required with 95% confidence limits within about 50% of the BER. Figure 14 shows that the 95% confidence limit (one-sided) will average 50% of the estimated BER if 13 errors were observed. Therefore, the required bit sample size is:

$$\frac{13}{1 \times 10^{-6}} = 13 \times 10^6 \text{ bits}$$

From this, a sample test time can be determined. For a bit rate of 12.55 Mb/s this is a sample duration of:

$$\frac{13 \times 10^6}{12.55 \times 10^6} = 1.1 \text{ seconds}$$

The same sample could be used to determine with 97.5% confidence (higher confidence) that the true BER was less than or equal to the estimated BER within 75% (larger tolerance). When the measurement is made, the number of errors observed may be more or less than the 13 expected, so the accuracy may be greater or less than desired. However, the above method does provide a starting point for determining sample size.

APPENDIX D

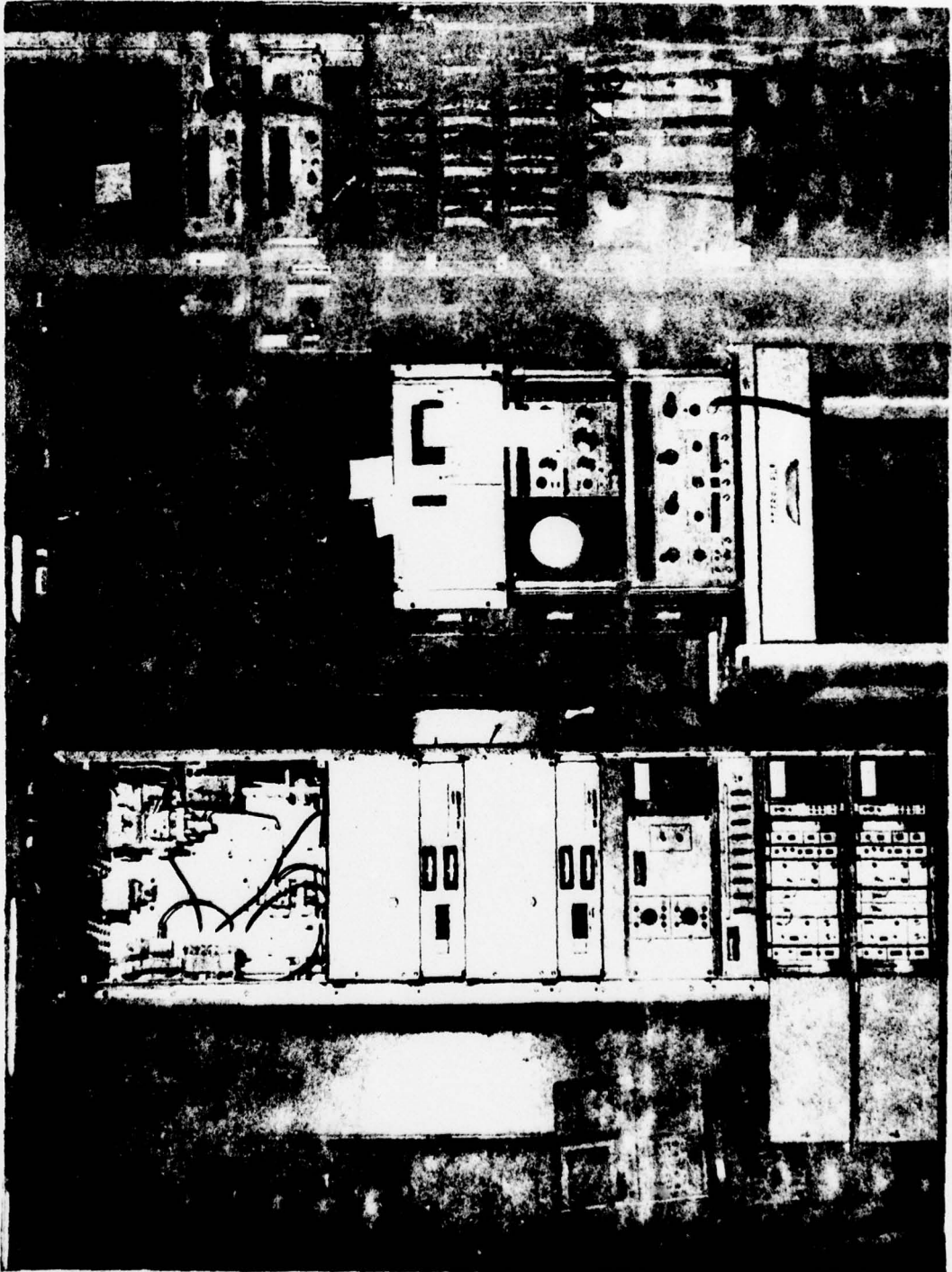


FIGURE 16. Photograph of DR8A

APPENDIX E

QUADRATURE PARTIAL RESPONSE THEORETICAL CURVE

Quadrature Partial Response (QPR) modulation is a combination of three-level partial response (3LPR) and phase shift keying (PSK) modulation. Derivations of 3LPR and PSK systems may be found separately in literature on data communications.³ A derivation of the expression for probability of error in terms of signal-to-noise (S/N) ratio for the DR8A QPR system was accomplished for USACEEIA by Dr. R. C. Jones, and by Richard Girvin, AFCS, Richards-Gebaur AFB. The critical parts of the analysis involve the following:

- a. Discussion of the low pass filter.
- b. Consideration of the average symbol power and the use of Parseval's Theorem.
- c. Expression in terms of the complementary error function.

The total low pass filter function is:

$$x(\omega) = T \cos(\omega T/2)$$

but it is divided equally among transmitter and receiver such that

$$G_T(\omega) = G_R(\omega) = X^{\frac{1}{2}}(\omega) = (T \cos(\omega T/2))^{\frac{1}{2}}$$

The time response is given by

$$x(t) = \frac{2}{\pi} \left\{ \frac{\cos(\pi t/T)}{1 - (2t/T)^2} \right\}$$

and it should be noted that an application of L'Hospital's Rule permits us to see that the limit of $X(t)$ as t approaches $\pm T/2$ is $\frac{1}{2}$.

We sample at $\pm T/2$, yielding:

$$X_n = X(nT - T/2) = \begin{cases} \frac{1}{2}, & n = 0, 1 \\ 0, & \text{otherwise} \end{cases}$$

We obtain an output of $Z_k = \frac{1}{2} a_k + \frac{1}{2} a_{k-1}$ with $Z_k = \pm d, 0$ as the three levels.

3. A Performance Monitoring Technique For Partial Response Transmission Systems, DCA, Reston, Virginia. (IEEE International Conference on Communications Conference Record, Vol 2, pp 40-14-19 ICC 73, June 11-13, Seattle, WA)

For the two channels the input is

$$s_{1,2}(t) = \sum_{j=-\infty}^{\infty} a_j x(t) u(t-jT/2)$$

where u is a step function.

The QPR form is

$$s(t) = s_1(t) \cos \omega_s t + s_2(t) \sin \omega_s t$$

Thus

$$s(t) = \sum_{j,k=-\infty}^{\infty} \{a_j x_1(t) u(t-jT/2) \cos \omega_s t + a_k x_2(t) u(t-kT/2) \sin \omega_s t\}$$

Ergodicity is assumed and

$$\bar{P}_s = \lim_{N \rightarrow \infty} (1/2NT) \int_{-NT}^{NT} \sum_{j,k} \sum_{l,m} \{s^2(t)\} dt$$

$$= \lim_{N \rightarrow \infty} \bar{a}_N^2 / N(T/2) \sum_{n=-N}^N \int_{-NT}^{NT} x^2(t) dt (u(t-nT/2))^2$$

$$= 4\bar{a}_N^2 / T \int_{-\infty}^{\infty} x^2(t) dt$$

Employing Parseval's Theorem

$$\bar{P}_s = 2\bar{a}_N^2 / \pi T \int_{-\infty}^{\infty} |X^2(\omega)|^2 d\omega$$

Since $X(\omega) = 0$ for $\omega > |\pi/T|$

$$\bar{P}_s = 2\bar{a}_N^2 / \pi T \int_{-\pi/T}^{\pi/T} |X^2(\omega)|^2 d\omega = 8\bar{a}_N^2 / \pi T$$

But $\bar{a}_N^2 = (d/2)^2 + (d/2)^2 = d^2/2$

$$\bar{P}_s = 4d^2 / \pi T$$

The noise power density in the pertinent band is

$$\begin{aligned} \bar{P}_N &\equiv \sigma^2 = 1/2\pi \int_{-\pi T}^{\pi T} N_0 |X^2(\omega)|^2 d\omega \\ &= 2N_0 / T \end{aligned}$$

The received levels in the absence of noise are d , 0 , $-d$ and the probabilities of receiving these are $\frac{1}{4}$, $\frac{1}{2}$, and $\frac{1}{4}$, respectively. Therefore

$$P_e = 3/2 P(\eta > d)$$

$$P_e = 3/2 Q(d/2\sigma)$$

where

$$Q(x) = 1/\sqrt{2\pi} \int_x^{\infty} e^{-t^2/2} dt$$

$$P_e = 3/2 Q\left\{\frac{1}{2} (P_s \pi^2 T / 8N_0)^{1/2}\right\}$$

$$= 3/2 Q\left\{\pi/4 (P_s T / 2N_0)^{1/2}\right\}$$

$$= 3/2 Q\left\{\pi/\sqrt{32} (S/N)^{1/2}\right\}$$

$$= 3/4 \operatorname{erfc}\left\{\pi/\sqrt{32} (S/N)^{1/2}\right\}$$

Where erfc is the complementary error function and

$$\operatorname{erfc}(x/\sqrt{2}) = 2/\sqrt{\pi} \int_{x/\sqrt{2}}^{\infty} e^{-\xi^2} d\xi$$

The scrambler/descrambler combination used in the DR8A multiplies the error rate of the decoder output by three, therefore:

$$P_e = 9/4 \operatorname{erfc}\left\{\pi/\sqrt{32} (S/N)^{1/2}\right\}$$

It is convenient to express the probability of error in terms of the energy per bit per noise spectral density (E_b/N_0) for comparison with other systems.

$$E_b = S/R \text{ where } R \text{ is the bit rate and } N = N_0/T$$

The bit rate, R may be expressed as $2/T$ and $S/N = E_b/N_0 \cdot 2$ so

$$P_e = 9/4 \operatorname{erfc}\left\{(\pi/4) (E_b/N_0)^{1/2}\right\}$$

Figure 17 is a plot of the probability of error expressed in terms of S/N . Figure 18 is a plot of BER expressed in terms of E_b/N_0 . To evaluate the expression for P_e , a fast complementary error function obtained by Dr. Jones from Lawrence Livermore Laboratory was used on the HP-9825 programmable calculator.

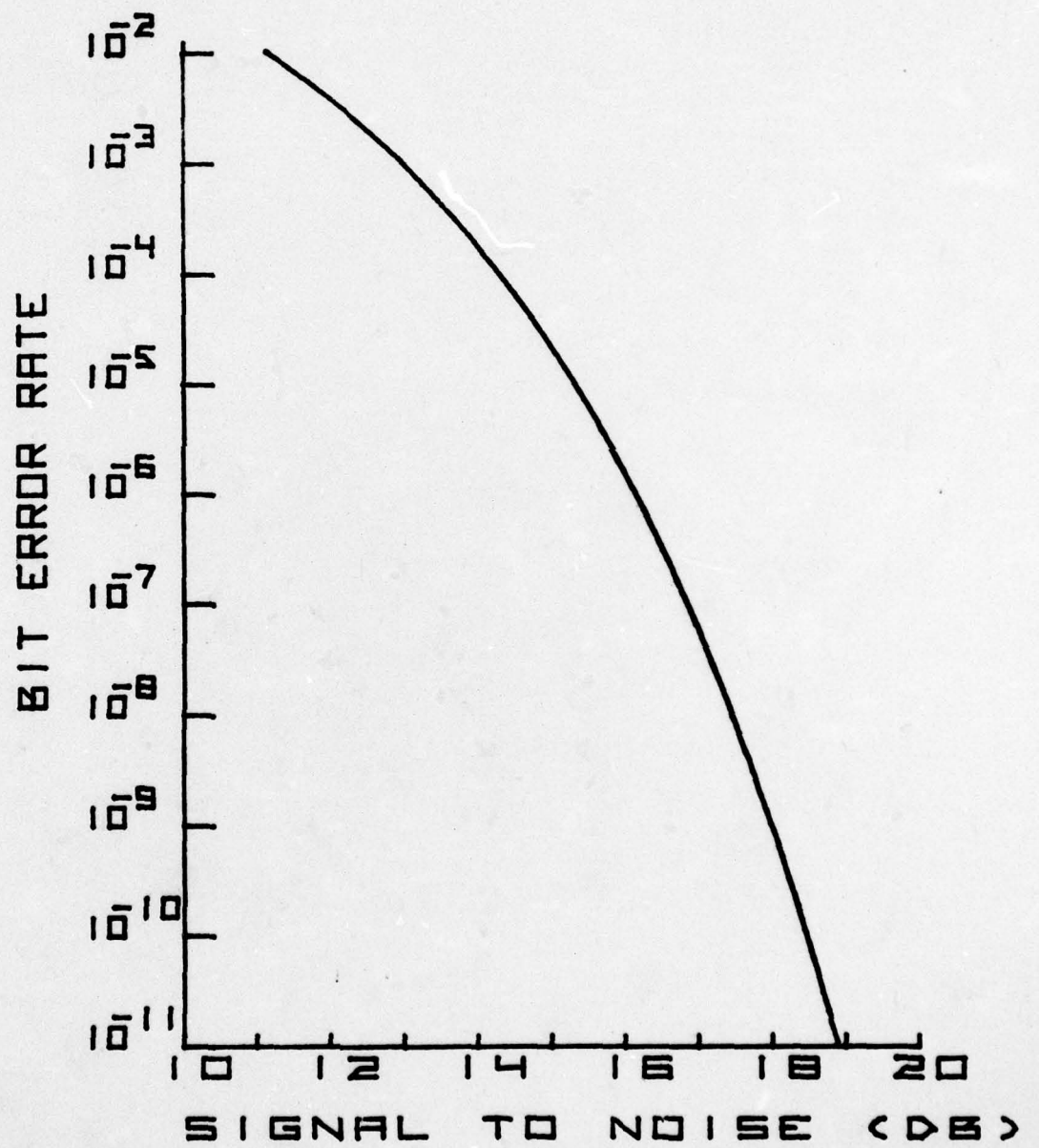


Figure 17. Quadrature Partial Response Theoretical Curve BER vs S/N

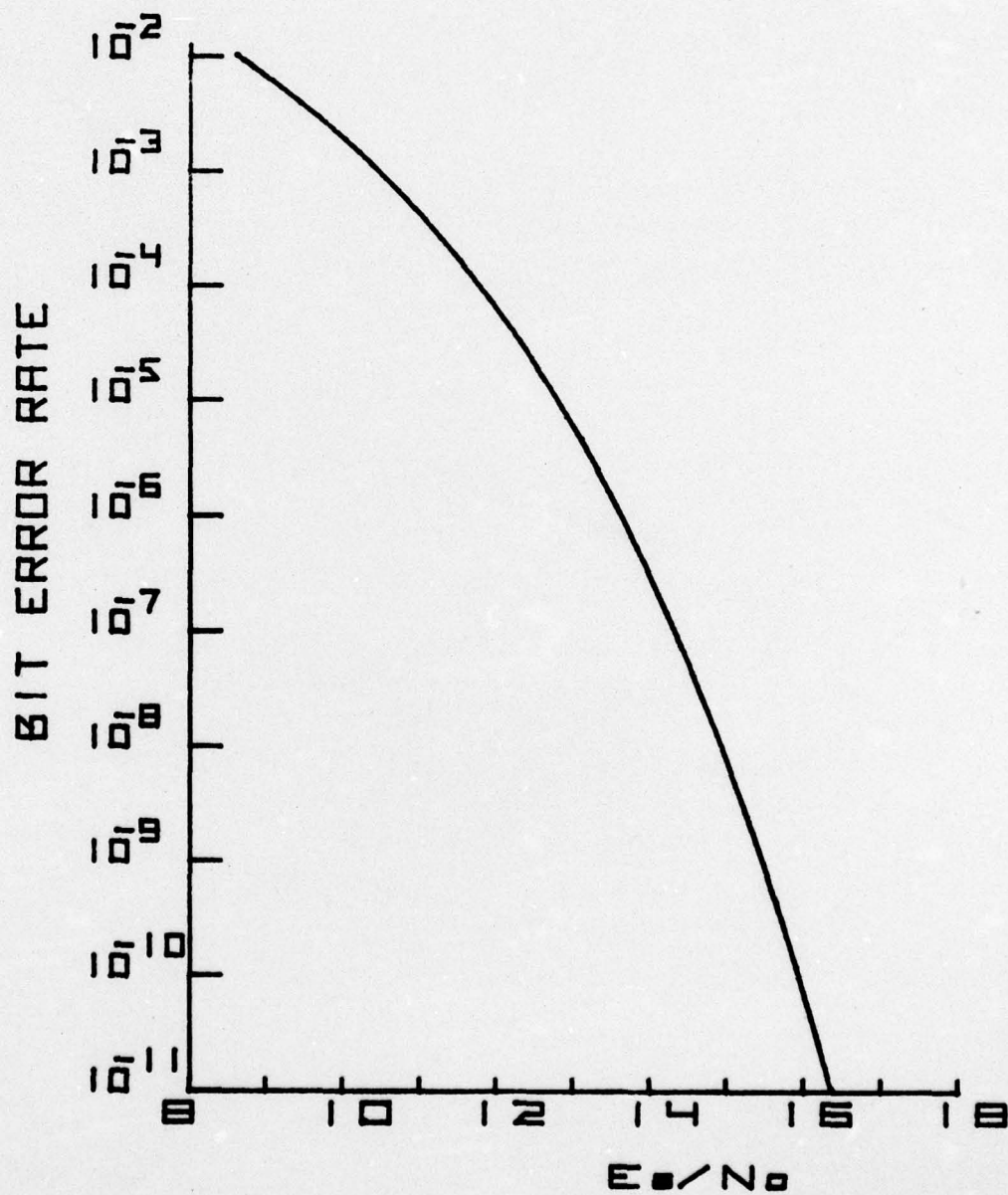


Figure 18. Quadrature Partial Response Theoretical Curve BER vs E_b/N_0

APPENDIX F

DIGITAL TRANSMISSION EVALUATION PROJECT REPORTS

<u>NUMBER</u>	<u>NAME</u>	<u>DATE</u>
ACCC-CED-74-DTEP-001	<u>RDS-80 Interim</u>	Oct 74
ACCC-CED-DTEP-LR1	<u>Vicom-MUX</u>	Dec 74
CCC-CED-74-DTEP-002	<u>MW-518(QPSK) Interim</u>	Dec 74
CCC-SR-75-DTEP-003	<u>Digital Industry Survey</u>	Jan 75
CCC-CED-75-DTEP-004	<u>RDS-80G Final</u>	Feb 75
CCC-CED-75-DTEP-005	<u>RDS-80 Final</u>	Mar 75
CCC-CED-75-DTEP-006	<u>AN/FRC 162 Interim</u>	Sep 75
CCC-SR-75-DTEP-007	<u>Equip Comparison Special</u>	Aug 75
CCC-CED-75-DTEP-008	<u>MW-518(QPSK) Final</u>	Oct 75
CCC-SR-75-DTEP-009	<u>23P2B Sensor Logic Switch</u>	Sep 75
CCC-CED-75-DTEP-010	<u>DR8A Interim</u>	Dec 75
CCC-CED-76-DTEP-011	<u>AN/FRC 162 Final</u>	May 76
CCC-CED-77-DTEP-012	<u>DR8A Final</u>	Apr 77
CCC-CED-76-DTEP-013	<u>Final Evaluation</u>	Jul 76
CCC-CED-76-DTEP-014	<u>DEB CONUS Link Interim</u>	Oct 76

DISTRIBUTION	<u>COPIES</u>
AFCS/EPES, Richards Gebaur AFB, MO 64030	2
AFTEC/TEEC, Kirtland AFB, NM 87115	1
CSAF, ATTN: RDPE, Washington, DC 20305	1
ATTN: PRCX, Washington, DC 20305	1
DA/DAMO-TCS-T, Washington, DC 20305	4
DCA, ATTN: NSA Liaison Office, Washington, DC 20305	1
ATTN: 430, Washington, DC 20305	1
ATTN: 470, Washington, DC 20305	1
DCEC, ATTN: R105, 1860 Wiehle Ave, Reston, VA 22070	2
ATTN: R220, 1860 Wiehle Ave, Reston, VA 22070	2
ATTN: R230, 1860 Wiehle Ave, Reston, VA 22070	2
ATTN: R710, 1860 Wiehle Ave, Reston, VA 22070	2
Defense Documentation Center, Alexandria, VA 22314	15
ECAC, ATTN: ACV, Mr. Mager, North Severn, Annapolis, MD 21402	3
Joint Tactical Communications Office,	
ATTN: TT-E-E, 197 Hance Rd, New Shrewsbury, NJ	1
ATTN: TT-E-S, 197 Hance Rd, New Shrewsbury, NJ	1
ATTN: TT-RT-TA, 197 Hance Road, New Shrewsbury, NJ	1
JTO, Tri-Tac, Fort Huachuca, AZ 85613	1
Mitre Corp., P. O. Box 208, ATTN: Mail Stop A160 Bedford, MA 01730	2
National Bureau of Standards, Electromagnetic Division ATTN: W. J. Aispach, Boulder, CO 80302	1
Naval Telecommunications Command,	
ATTN: 3426, Massachusetts Avenue, NW, Wash. DC 20390	1
ATTN: 4401, Massachusetts Avenue, NW, Wash. DC 20390	1
NCA/EPE, Griffis AFB, NY 13440	2
NSA, ATTN: Code R15, Fort Meade, MD 20755	1
ATTN: Code S254, Fort Meade, MD 20755	1
ATTN: Code 4023, Fort Meade, MD 20755	2

RADC, ATTN: DCLD, Griffis AFB, NY 13440	2
ATTN: DCC, Griffis AFB, NY 13440	1
USACC, ATTN: CC-OPS-SM, Fort Huachuca, AZ 85613	4
ATTN: CC-OPS-ST, Fort Huachuca, AZ 85613	2
USACEEIA, ATTN: CCC-CED, Fort Huachuca, AZ 85613	10
ATTN: CCC-TCO, Fort Huachuca, AZ 85613	2
ATTN: CCC-TED, Fort Huachuca, AZ 85613	5
ATTN: CCC-PRSO, Fort Huachuca, AZ 85613	2
USACSA: ATTN: CCM-CCS, Fort Monmouth, NJ 07703	1
ATTN: CCM-SG, Fort Huachuca, AZ 85613	1
ATTN: CCM-RD, Fort Monmouth, NJ 07703	1
US Department of Commerce, Office of Telecommunications, Institute for Telecommunications Sciences, ATTN: Richard Skerjanec, Boulder, CO 80302	2
USAECOM, ATTN: AMSEL-NL-P3, Fort Monmouth NJ 07703	1
ATTN: AMSEL-NL-D, Fort Monmouth, NJ 07703	1
USAEPG/STEEP-MT-GT, Fort Huachuca, AZ 85613	4
ESD, ATTN: DCF Hanscom AFB, Mass 01731	2